



# Atmospheric CO and CH<sub>4</sub> time series and seasonal variations on Reunion Island from ground-based in situ and FTIR (NDACC and TCCON) measurements

Minqiang Zhou<sup>1</sup>, Bavo Langerock<sup>1</sup>, Corinne Vigouroux<sup>1</sup>, Mahesh Kumar Sha<sup>1</sup>, Michel Ramonet<sup>2</sup>, Marc Delmotte<sup>2</sup>, Emmanuel Mahieu<sup>3</sup>, Whitney Bader<sup>3</sup>, Christian Hermans<sup>1</sup>, Nicolas Kumps<sup>1</sup>, Jean-Marc Metzger<sup>4</sup>, Valentin Duflot<sup>5,4</sup>, Zhiting Wang<sup>6,7</sup>, Mathias Palm<sup>6</sup>, and Martine De Mazière<sup>1</sup>

<sup>1</sup>Royal Belgian Institute for Space Aeronomy (BIRA-IASB), Brussels, Belgium

<sup>2</sup>Laboratoire des Sciences du Climat et de l'Environnement (LSCE/IPSL), UMR CEA-CNRS-UVSQ, Gif-sur-Yvette, France

<sup>3</sup>Institut d'Astrophysique et de Géophysique, Université de Liège, Liège, Belgium

<sup>4</sup>UMS 3365 – OSU Réunion, Université de La Réunion, Saint-Denis, Réunion, France

<sup>5</sup>Laboratoire de l'Atmosphère et des Cyclones (LACy), UMR8105, Saint-Denis, Réunion, France

<sup>6</sup>Institute of Environmental Physics, University of Bremen, Bremen, Germany

<sup>7</sup>College of Atmospheric Science, Lanzhou University, Lanzhou 730000, China

**Correspondence:** Minqiang Zhou (minqiang.zhou@aeronomie.be)

Received: 28 February 2018 – Discussion started: 17 May 2018

Revised: 27 August 2018 – Accepted: 11 September 2018 – Published: 1 October 2018

**Abstract.** Atmospheric carbon monoxide (CO) and methane (CH<sub>4</sub>) mole fractions are measured by ground-based in situ cavity ring-down spectroscopy (CRDS) analyzers and Fourier transform infrared (FTIR) spectrometers at two sites (St Denis and Maïdo) on Reunion Island (21° S, 55° E) in the Indian Ocean. Currently, the FTIR Bruker IFS 125HR at St Denis records the direct solar spectra in the near-infrared range, contributing to the Total Carbon Column Observing Network (TCCON). The FTIR Bruker IFS 125HR at Maïdo records the direct solar spectra in the mid-infrared (MIR) range, contributing to the Network for the Detection of Atmospheric Composition Change (NDACC). In order to understand the atmospheric CO and CH<sub>4</sub> variability on Reunion Island, the time series and seasonal cycles of CO and CH<sub>4</sub> from in situ and FTIR (NDACC and TCCON) measurements are analyzed. Meanwhile, the difference between the in situ and FTIR measurements are discussed.

The CO seasonal cycles observed from the in situ measurements at Maïdo and FTIR retrievals at both St Denis and Maïdo are in good agreement with a peak in September–November, primarily driven by the emissions from biomass burning in Africa and South America. The dry-air column averaged mole fraction of CO ( $X_{\text{CO}}$ ) derived from the FTIR

MIR spectra (NDACC) is about 15.7 ppb larger than the CO mole fraction near the surface at Maïdo, because the air in the lower troposphere mainly comes from the Indian Ocean while the air in the middle and upper troposphere mainly comes from Africa and South America. The trend for CO on Reunion Island is unclear during the 2011–2017 period, and more data need to be collected to get a robust result.

A very good agreement is observed in the tropospheric and stratospheric CH<sub>4</sub> seasonal cycles between FTIR (NDACC and TCCON) measurements, and in situ and the Michelson Interferometer for Passive Atmospheric Sounding (MIPAS) satellite measurements, respectively. In the troposphere, the CH<sub>4</sub> mole fraction is high in August–September and low in December–January, which is due to the OH seasonal variation. In the stratosphere, the CH<sub>4</sub> mole fraction has its maximum in March–April and its minimum in August–October, which is dominated by vertical transport. In addition, the different CH<sub>4</sub> mole fractions between the in situ, NDACC and TCCON CH<sub>4</sub> measurements in the troposphere are discussed, and all measurements are in good agreement with the GEOS-Chem model simulation. The trend of  $X_{\text{CH}_4}$  is  $7.6 \pm 0.4 \text{ ppb yr}^{-1}$  from the TCCON measurements over the 2011 to 2017 time period, which is consistent with the CH<sub>4</sub>

trend of  $7.4 \pm 0.5 \text{ ppb yr}^{-1}$  from the in situ measurements for the same time period at St Denis.

## 1 Introduction

Carbon monoxide (CO) is a colorless and poisonous trace gas, which contributes significantly to the pollution of our planet. CO has a lifetime of several weeks to a few months (Novelli et al., 1998); therefore, it is generally used in atmospheric sciences as a tracer to study the long-distance transport of forest fire, biomass burning and other emissions (Duflot et al., 2010). CO also plays an important role in atmospheric chemistry, especially as it reacts with hydroxyl radicals (OH) that affect the carbon and the methane (CH<sub>4</sub>) cycles (Rasmussen and Khalil, 1981) and take part in the formation of many other polluting gases, e.g., tropospheric ozone and urban smog (Aschi and Largo, 2003). CH<sub>4</sub> is the second most important anthropogenic greenhouse gas after carbon dioxide (CO<sub>2</sub>), with a global warming potential about 28 times greater than CO<sub>2</sub> over a 100-year time horizon. About 17 % of the total increase in radiative forcing between 1750 and 2010 related to the long-lived greenhouse gases in the atmosphere is caused by CH<sub>4</sub> (IPCC, 2013). In addition, CH<sub>4</sub> also reacts with OH, affecting the atmospheric oxidizing capacity. CH<sub>4</sub> is well-mixed in the lower atmosphere with a life time of 8–10 years (Kirschke et al., 2013).

In recent decades, CH<sub>4</sub> growth rates in the atmosphere have been variable. The CH<sub>4</sub> concentration increased in the 1990s at a rate of  $0.7\% \text{ yr}^{-1}$ , it was then relatively stable in the first half of the 2000s, and then started increasing again after 2007 (Rigby et al., 2008). The CO concentration increased from the 1950s and then started to decrease in the late 1980s (Novelli, 2003). The importance of CO and CH<sub>4</sub> in our changing atmosphere motivates continuous and long-term time series of precise and accurate measurements of these species. Several kinds of measurement techniques have been used to monitor the CO and CH<sub>4</sub> mole fractions in the atmosphere, e.g., ground-based in situ or sampling measurements (Vermeulen et al., 2011; Lopez et al., 2015), ground-based Fourier transform infrared (FTIR) spectrometer observations (Sussmann et al., 2012; Té et al., 2016), and space-based satellite measurements such as the Michelson Interferometer for Passive Atmospheric Sounding (MIPAS), the Greenhouse gases Observing SATellite (GOSAT) and the Measurement Of Pollution In The Troposphere (MOPITT) (von Clarmann et al., 2003; Yokota et al., 2009; Deeter et al., 2014). In addition to providing useful means for trend determination, such measurements allow the verification of atmospheric models for air pollution and climate change, e.g., Té et al. (2016) used ground-based in situ and FTIR measurements as well as GEOS-Chem simulations to explain the seasonal variability of atmospheric CO, and Bader et al. (2017) used FTIR measurements and the GEOS-Chem model to investigate the

possible causes for the increase of atmospheric CH<sub>4</sub> since 2005.

Reunion Island is a unique atmospheric observatory situated in the Indian Ocean, about 700 km east of Madagascar and 170 km southwest of Mauritius. It is one of the very few atmospheric observation stations that provides both in situ and remote sensing FTIR CO and CH<sub>4</sub> data in the Southern Hemisphere. Both in situ and FTIR measurement techniques are capable of measuring CO and CH<sub>4</sub> mole fractions with high accuracy and precision; therefore, they are good candidates to study the changes in atmospheric compositions, and to trace the emissions. However, using ground-based in situ and FTIR measurements requires a good understanding of the uncertainty and representativeness of each dataset. In situ instruments monitor gas mole fractions near the surface, while FTIR retrievals report information on the distribution of the gas abundance with altitude. The representativeness of both measurements depends on the location of the site, the air transport and the lifetime of the target species (Folini et al., 2009; Dils et al., 2011; Sepúlveda et al., 2014). In addition, the representativeness of FTIR retrievals, and their vertical sensitivity is also related to the spectral range and retrieval strategy, which has to be taken into account when comparing the Total Carbon Column Observing Network (TCCON) and the Detection of Atmospheric Composition Change (NDACC) data (Ostler et al., 2014; Kiel et al., 2016).

The objective of this paper is to study the atmospheric CO and CH<sub>4</sub> time series and seasonal variations on Reunion Island based on the in situ and FTIR measurements from two sites: Saint Denis (St Denis) and Maïdo. The different ground-based in situ and FTIR techniques (NDACC and TCCON) are used to show their complementarity with regards to obtaining the CO and CH<sub>4</sub> abundances at the surface and in the troposphere and stratosphere. Section 2 introduces the datasets at the two sites. The measurement uncertainty and characterization of the various datasets are also presented. In the next section, the time series and seasonal cycles of CO and CH<sub>4</sub> from the in situ measurements at the surface and FTIR column retrievals are analyzed. In addition, intercomparisons between colocated daily means of the in situ and FTIR measurements are carried out. In Sect. 4, the differences of CO and CH<sub>4</sub> between the in situ and FTIR measurements are discussed using the vertical information from the FTIR data which allows tropospheric columns to be derived, and by providing GEOS-Chem model comparisons for CH<sub>4</sub> in the troposphere. Furthermore, in Sect. 4, the FTIR CH<sub>4</sub> stratospheric columns are compared with MIPAS satellite data. Finally, conclusions are drawn in Sect. 5.

## 2 Measurements on Reunion Island

There are two sites on Reunion Island: St Denis ( $-20.9014^\circ \text{ N}, 55.4848^\circ \text{ E}$ ; 85 m a.s.l. above sea level) which

is close to the coast, and Maïdo ( $-21.0796^{\circ}$  N,  $55.3841^{\circ}$  E; 2155 m a.s.l.) which is close to the top of the mountain ridge. Table 1 lists all of the available CO and CH<sub>4</sub> measurements from these two sites, in addition to their measurement uncertainties. Currently, each site is operated with a FTIR instrument and an in situ cavity ring-down spectroscopy (CRDS) analyzer. In this section, we give a brief historic overview of the in situ and the FTIR measurements on Reunion Island.

## 2.1 In situ measurements

The Royal Belgian Institute for Space Aeronomy (BIRA-IASB) in collaboration with the Laboratoire de l'Atmosphère et des Cyclones (LACy), the Observatoire des Sciences de l'Univers de la Réunion (OSU-R) and the Laboratoire des Sciences du Climat et de l'Environnement (LSCE), has been performing in situ surface measurements on Reunion Island. The CH<sub>4</sub> mole fraction has been measured by a CRDS analyzer (Picarro G1301) at St Denis since August 2010, and CO and the CH<sub>4</sub> mole fractions have been collected by another CRDS analyzer (Picarro G2401) at Maïdo since December 2014. The latter installation will be proposed for a certification (to be certified for standardized data production) in the European research infrastructure Integrated Carbon Observation System (ICOS-ERIC) as a French-Belgian station in late 2018. The St Denis coastal site has been developed within the French national monitoring network. The two stations have been set up in a similar way, taking the technical specifications recommended by ICOS into account (Laurent, 2016). Both CRDS analyzers are calibrated every 3 to 4 weeks with a suite of four cylinders that have concentrations spanning the atmospheric ranges of CH<sub>4</sub> and CO, and have been calibrated at LSCE with NOAA reference tanks. All values are expressed in WMO reference scales (X2004A and X2014A for CH<sub>4</sub> and CO, respectively). In addition, these tanks are used to calculate the continuous monitoring repeatability (CMR) and the long-term repeatability (LTR) as defined by Yver Kwok et al. (2015). The air is sampled through a 1/4" tube ("Synflex 3000") at the top of the building, and goes through a 2 µm filter, and a multi-position valve before being analyzed by the CRDS analyzer. The pump is always located downstream of the analyzer. Raw data are transferred to the LSCE server every night, and are processed according to the ICOS specifications (Hazan et al., 2016). The in situ measurements at the two surface sites are carried out in wet conditions without any dryer in the sampling line. The correction of the dry air mole fractions is carried out using the H<sub>2</sub>O measurements performed by the same analyzers (Rella et al., 2013).

## 2.2 FTIR instruments

In 2002 (October) and 2004 (August to November), BIRA-IASB carried out two atmospheric monitoring experiments using a mobile Bruker IFS 120M FTIR equipped with indium

antimonide (InSb) and mercury cadmium telluride (MCT) detectors at St Denis on the campus of the Université de La Réunion (Senten et al., 2008). The same instrument was operated at St Denis to provide continuous measurements between June 2009 and November 2011 (Vigouroux et al., 2012; Zhou et al., 2016). The instrument recorded the solar spectra in the mid-infrared (MIR) range from 600 to 4500 cm<sup>-1</sup>, contributing to the NDACC network.

In September 2011, BIRA-IASB installed a high-resolution Bruker IFS 125HR FTIR at St Denis next to the FTIR 120M. This instrument is primarily dedicated to measuring the near-infrared (NIR: 4000–16 000 cm<sup>-1</sup>) spectra, with silicon (Si) and indium gallium arsenide (InGaAs) detectors, and contributes to TCCON.

In March 2013, BIRA-IASB started operating a second Bruker IFS 125HR FTIR spectrometer, observing the MIR spectra with MCT and InSb detectors at the Maïdo observatory (Baray et al., 2013). These FTIR measurements are also affiliated with NDACC.

## 2.3 FTIR retrieval techniques

The optimal estimation method (Rodgers, 2000) is applied to retrieve the gas mole fractions from the FTIR solar spectra. The retrieval strategies are determined by the spectral range and the network (see Table 2).

### 2.3.1 TCCON

The TCCON (NIR) spectra at St Denis are analyzed using the GGG2014 algorithm to retrieve CO and CH<sub>4</sub> total columns (De Maziere et al., 2017). The details of the TCCON retrieval settings were described in Wunch et al. (2015). Note that GGG2014 applies a profile scaling; therefore, TCCON only provides a total column instead of a vertical profile. The daily a priori profiles are generated by a stand alone tool based on in situ and aircraft measurements (Toon and Wunch, 2014). Figure 1 shows the a priori profiles of CO and CH<sub>4</sub> at St Denis on four days in 2013. TCCON CO and CH<sub>4</sub> retrieved products have been calibrated and validated by Infrastructure for the Measurement of the Europe Carbon Cycle (IMECC) profiles over the European TCCON stations (Messerschmidt et al., 2011) and HIAPER Pole-to-Pole Observations (HIPPO) profiles over Northern America, East Asia and Oceania (Wunch et al., 2010); the calibration factors (CO:  $1.067 \pm 0.020$ ; CH<sub>4</sub>:  $0.977 \pm 0.002$ ) are found to be robust both over time and from site to site (Wunch et al., 2015). The data in this study have all been corrected by applying these calibration factors. Therefore, it is assumed that there are no systematic uncertainties for the TCCON retrievals, and only random uncertainties are listed in Table 1.

Figure 2 shows the column averaging kernels (AVK) of TCCON CO and CH<sub>4</sub> retrievals for different solar zenith angles (SZAs). At St Denis, the SZA is mainly in the range from 20 to 70°. The AVK represents the sensitivity of the

**Table 1.** In situ and FTIR CO and CH<sub>4</sub> measurements at St Denis and Maïdo.

Site	St Denis			Maïdo	
Location	–20.9014 N, 55.4848 E			–21.0796 N, 55.3841 E	
Altitude	85 m a.s.l.			2155 m a.s.l.	
Instrument	FTIR IFS 120M	FTIR IFS 125HR	Picarro G1301	FTIR IFS 125HR	Picarro G2401
Time coverage	10.2002–11.2001	9.2011–present	8.2010–present	3.2013–present	1.2014–present
Network	NDACC	TCCON	French atmospheric monitoring network	NDACC	ICOS applicant
CO uncertainty*	2.7/1.2 %	–/1.2 %	–	2.5/1.0 %	–/1.5 ppb
CH <sub>4</sub> uncertainty*	3.5/1.6 %	–/0.5 %	–/2.0 ppb	3.0/1.5 %	–/0.5 ppb

\* FTIR uncertainty is in relative units, while in situ uncertainty is in absolute units of VMR. NDACC uncertainty is reported on the total column, and it is separated into two components (systematic/random). TCCON uncertainty is reported on the total column-averaged mole fraction. TCCON and in situ measurements have been validated with WMO standards, so it is assumed there are no systematic uncertainties for these data.

**Table 2.** NDACC and TCCON CO and CH<sub>4</sub> retrieval strategies for data recorded on Reunion Island.

Species	CO		CH <sub>4</sub>	
Network	TCCON	NDACC	TCCON	NDACC
Algorithm	GGG2014	SFIT4	GGG2014	SFIT4
Retrieval windows (cm <sup>–1</sup> )	4208.7–4257.3 4262.0–4318.8	2057.7–2058.0 2069.56–2069.76 2157.5–2159.15	5872.0–5988.0 5996.45–6007.55 6007.0–6145.0	2611.6–2613.35 2613.7–2615.4 2835.55–2835.8 2903.82–2903.925 2941.51–2942.22
Interfering species	CH <sub>4</sub> , H <sub>2</sub> O and HDO	O <sub>3</sub> , N <sub>2</sub> O, H <sub>2</sub> O, OCS and CO <sub>2</sub>	CO <sub>2</sub> , H <sub>2</sub> O and N <sub>2</sub> O,	H <sub>2</sub> O, HDO, CO <sub>2</sub> and NO <sub>2</sub>
Spectroscopy	ATM	ATM	ATM	DLR H <sub>2</sub> O, ATM
A priori profile	TCCON tool (daily)	WACCM v4 (fixed)	TCCON tool (daily)	WACCM v4 (fixed)
Retrieval constraint	Scaling of a priori profile	Optimal estimation DOF = 2.0 ± 0.2 (St Denis) DOF = 2.3 ± 0.2 (Maïdo)	Scaling of a priori profile	Optimal estimation DOF = 2.1 ± 0.2 (St Denis) DOF = 2.5 ± 0.3 (Maïdo)
Products	Total column	Profile	Total column	Profile

retrieved total column to the true partial column profile. Ideally, the AVK should be 1.0 at all altitudes, meaning that the retrieved total column is the same as the true column, with a perfect sensitivity to the whole atmosphere. However, in reality, the AVK is not always equal to 1.0. If the value is larger than 1.0 at an altitude, it means that the retrieved total column overestimates the contribution from that particular layer in the total column budget, and vice versa. As a result, the TCCON retrieved CO total column underestimates a deviation from the a priori in the lower troposphere, and overestimates it at high altitudes. The TCCON retrieved CH<sub>4</sub> total column is more sensitive to the whole troposphere and stratosphere.

### 2.3.2 NDACC

The NDACC (MIR) spectra at St Denis and Maïdo are analyzed with the SFIT4 algorithm, an evolution of SFIT2 (Pougatchev et al., 1995), to retrieve the profiles of CO and CH<sub>4</sub>. The H<sub>2</sub>O a priori profile is extracted from the National

Centers for Environmental Prediction (NCEP) 6-hourly reanalysis data, and a priori profiles of other species are derived from the Whole Atmosphere Community Climate Model (WACCM) version 4 (see Fig. 1). In order to reduce the influence from the interfering species, profiles of O<sub>3</sub> and N<sub>2</sub>O and columns of H<sub>2</sub>O, OCS and CO<sub>2</sub> are simultaneously retrieved in addition to the CO profile (see Table 2). Profiles of H<sub>2</sub>O and HDO, and columns of CO<sub>2</sub> and NO<sub>2</sub> are simultaneously retrieved in addition to the CH<sub>4</sub> profile. The retrieval uncertainty of NDACC retrievals at Maïdo is slightly lower than that at St Denis, due to the higher signal-to-noise-Ratio (SNR) of the FTIR 125HR compared to the FTIR 120M. In addition, the H<sub>2</sub>O at Maïdo is less significant than that at St Denis due to the higher altitude, which is an important interfering species for CO and CH<sub>4</sub> retrievals. The NDACC retrievals are performed using the same atmospheric line list (ATM) (Toon, 2014) used by TCCON with the exception of the H<sub>2</sub>O line list (Birk et al., 2017;

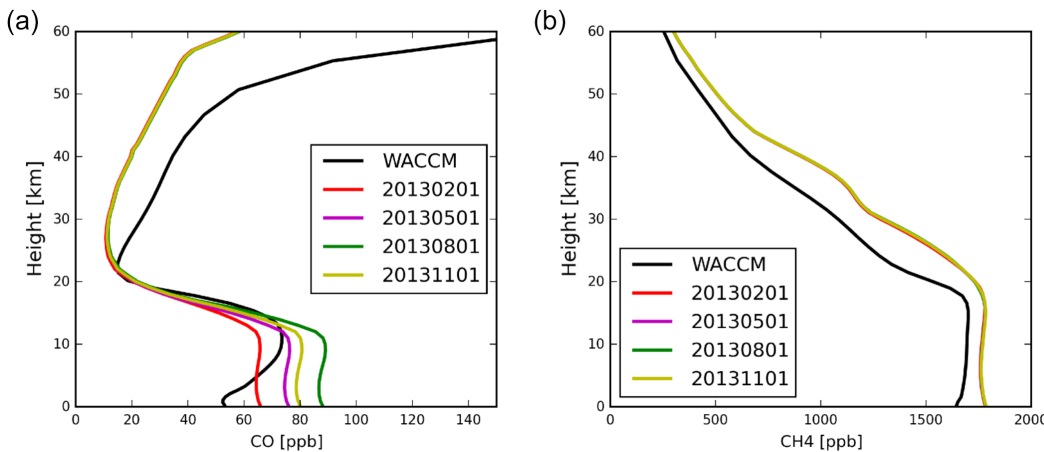


**Figure 1.** The a priori profiles used for TCCON measurements on 20130201 (year, month and day), 20130501, 20130801, 20131101 and NDACC measurements for CO (a) and CH<sub>4</sub> (b). Note that NDACC uses a fixed a priori profile from WACCM model for all retrievals.

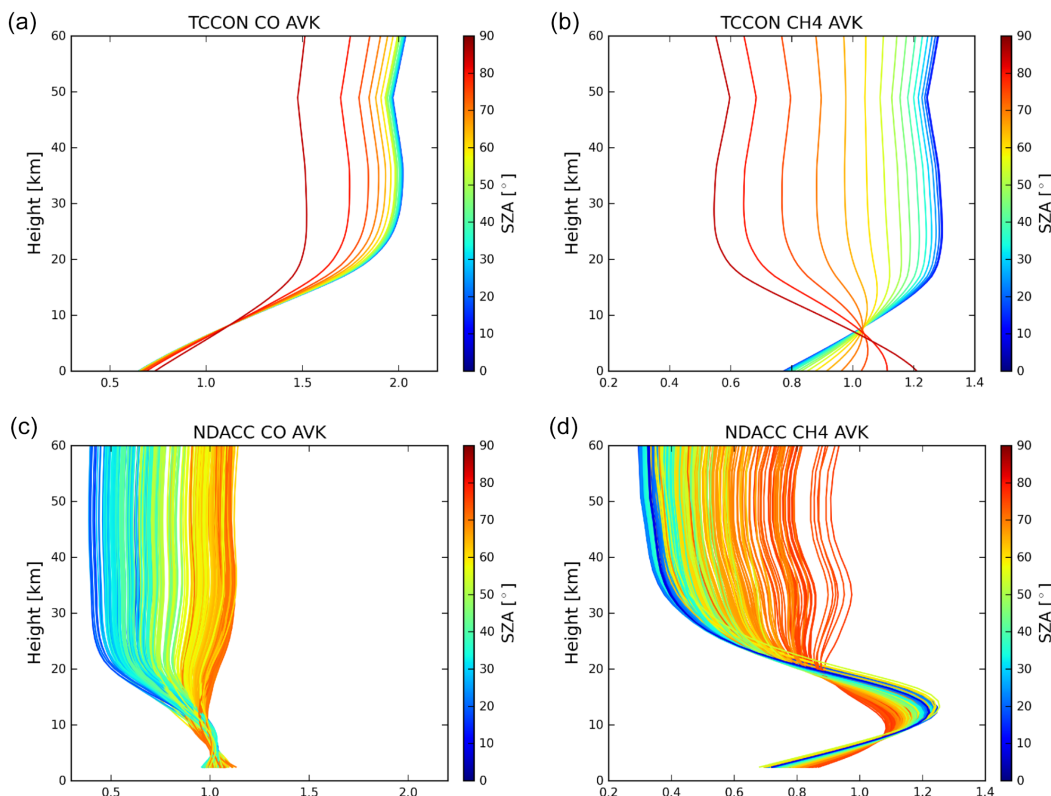


**Figure 2.** The top panels are the column averaging kernels of TCCON CO (a) and CH<sub>4</sub> (b) retrievals; the lower panels are the column averaging kernels of NDACC CO (c) and CH<sub>4</sub> (d) retrievals. All averaging kernels vary with the solar zenith angle (SZA). Note that the ranges of the x axes for CO and CH<sub>4</sub> are different.

Loos et al., 2017a, b) provided by the German Aerospace Center (DLR) in 2016 is adopted for NDACC CH<sub>4</sub> retrievals, which allows us to get a better spectral fitting.

The AVK for NDACC CO and CH<sub>4</sub> retrievals are shown in Fig. 2. Similar to TCCON, NDACC CO and CH<sub>4</sub> AVK vary

with SZA. NDACC CO retrievals have a good sensitivity to the whole troposphere and lower stratosphere. For CH<sub>4</sub>, the total column is sensitive to the whole troposphere and stratosphere. Apart from the total column, NDACC provides some profile information of CO and CH<sub>4</sub>. Figure 3 shows a typi-

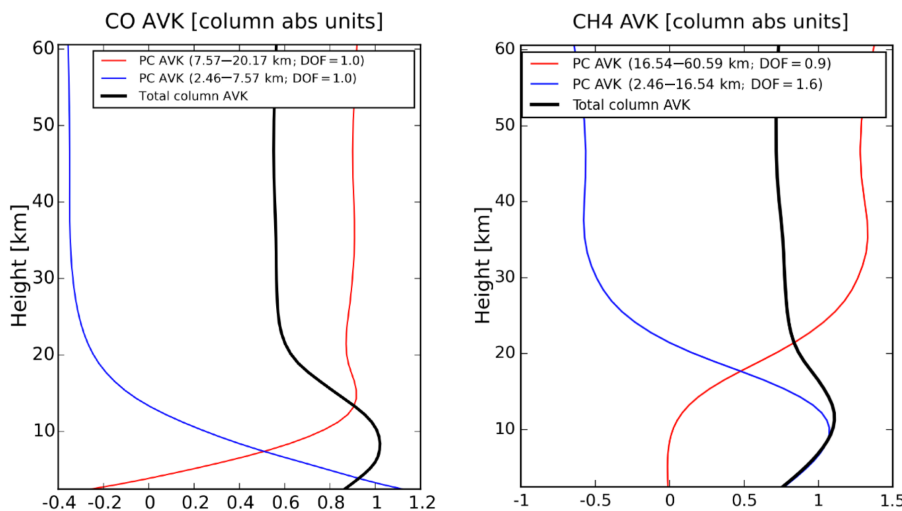


**Figure 3.** The total column averaging kernel (black) and the partial column averaging kernels of two individual layers (CO: surface–8 km and 8–20 km; CH<sub>4</sub>: surface–16 km and 16–60 km) of one typical NDACC retrieval at Maïdo.

cal AVK of CO and CH<sub>4</sub> NDACC retrievals at Maïdo. The averaged degrees of freedom for the signal (DOFs) of CO is  $2.0 \pm 0.2$  ( $1\sigma$ ) at St Denis and  $2.3 \pm 0.2$  ( $1\sigma$ ) at Maïdo, indicating that there are two individual layers of information (surface–8 km and 8–20 km) with the first layer having a strong sensitivity to the boundary layer. For CH<sub>4</sub>, the averaged DOFs of CH<sub>4</sub> is  $2.1 \pm 0.2$  ( $1\sigma$ ) at St Denis and  $2.5 \pm 0.3$  ( $1\sigma$ ) at Maïdo, indicating that there are also two individual layers of information (about surface–16 km and 16–60 km).

### 3 Comparison between the ground-based in situ and the FTIR total column measurements

#### 3.1 Methodology

In this section, we compare the CO and CH<sub>4</sub> dry air volume mixing ratio (VMR) observed by in situ measurements at the surface, with the dry-air column-averaged mole fractions ( $X_{\text{gas}}$ ) of FTIR (NDACC and TCCON) retrievals. For TCCON products, the O<sub>2</sub> total column is simultaneously retrieved with the target species. Since atmospheric O<sub>2</sub> mole fractions are considered stable with a VMR of 0.2095, the  $X_{\text{gas}}$  is calculated using the ratio between the total column of target species (TC<sub>gas</sub>) and O<sub>2</sub> (TC<sub>O<sub>2</sub></sub>):

$$X_{\text{gas}} = 0.2095 \frac{\text{TC}_{\text{gas}}}{\text{TC}_{\text{O}_2}}. \quad (1)$$

The advantage of dividing by O<sub>2</sub> abundance is that it reduces the systematic uncertainties from the parameters, which have a similar effect on the retrievals of both species, e.g., instrument line shape (ILS) and the SZA (Yang et al., 2002). For NDACC spectra, there are no N<sub>2</sub> or O<sub>2</sub> absorption windows that allow a sufficient accuracy of abundance to be achieved. Therefore, we use the dry-air total column (TC<sub>air</sub><sup>dry</sup>) to calcu-

late the  $X_{\text{gas}}$ :

$$X_{\text{gas}} = \frac{\text{TC}_{\text{gas}}}{\text{TC}_{\text{air}}^{\text{dry}}}, \quad (2)$$

$$\text{TC}_{\text{air}}^{\text{dry}} = \frac{P_s}{g m_{\text{air}}^{\text{dry}}} - \text{TC}_{\text{H}_2\text{O}}(m_{\text{H}_2\text{O}}/m_{\text{air}}^{\text{dry}}), \quad (3)$$

where  $P_s$  is the surface pressure;  $g$  is the column-averaged gravitational acceleration;  $m_{\text{H}_2\text{O}}$  and  $m_{\text{air}}^{\text{dry}}$  are the molecular mass of H<sub>2</sub>O and dry air, respectively; and TC<sub>H<sub>2</sub>O</sub> is the total column of H<sub>2</sub>O from NCEP reanalysis data. The surface pressures at St Denis and Maïdo are recorded by Vaisala PTB210 sensors, with an accuracy better than 0.1 hPa. The systematic uncertainty of H<sub>2</sub>O in the troposphere is about 5 %, and the TC<sub>H<sub>2</sub>O</sub> on Reunion Island is about 0.5 %–2 % of the TC<sub>air</sub>. Consequently, the uncertainty of the TC<sub>air</sub><sup>dry</sup> is less than 0.1 %.

A regression model is applied to derive the trends of CO and CH<sub>4</sub>, which has been described in Zhou et al. (2018):

$$Y(t) = A_0 + A_1 \cdot t + \sum_{k=1}^3 (A_{2k} \cos(2k\pi t) + A_{2k+1} \sin(2k\pi t)) + \varepsilon(t), \quad (4)$$

where  $A_0$  is the intercept,  $A_1$  is the annual growth rate,  $A_2$  to  $A_7$  are the periodic variations,  $\varepsilon(t)$  is the residual between the measurements and the fitting model, and  $Y(t)$  is measurements with the  $t$  in fraction of year. After that, the detrended monthly means of the measurements are applied to obtain the seasonal variation, and the uncertainty ( $2\sigma/\sqrt{n}$ ;  $\sigma$  and  $n$  are the standard deviation and the number of the measurements for each month).

For more quantitative comparisons, we also use the collocated daily means from the in situ and FTIR measurements at

each site (St Denis: CH<sub>4</sub>; Maïdo: CO and CH<sub>4</sub>). Note that the FTIR instrument measures direct sunlight, and it depends on clear sky conditions. Therefore, we filter the in situ measurements to daytime measurements (06:00–18:00 local time) to reduce the impact of the diurnal variation.

### 3.2 CO

The time series and seasonal cycle of CO from the in situ and FTIR measurements are shown in Figs. 4–5. For each dataset, we use all the available data to get a robust detrended time series and then to obtain the seasonal cycle. Figure 4 shows that the TCCON  $X_{\text{CO}}$  at St Denis is in good agreement with the NDACC  $X_{\text{CO}}$  at Maïdo, while the in situ CO observations at Maïdo are generally lower than the FTIR measurements with the exception of few higher peaks. There is no distinct  $X_{\text{CO}}$  trend derived from both FTIR datasets (TCCON:  $-0.09 \pm 1.1 \text{ ppb yr}^{-1}$  ( $2\sigma$ ) for the 2011–2017 period; NDACC:  $-1.16 \pm 2.08 \text{ ppb yr}^{-1}$  for 2013–2017), while a slight decreasing trend ( $-4.66 \pm 3.16 \text{ ppb yr}^{-1}$ ) is derived from the in situ measurements for the 2015–2017 period. The large uncertainty of the decreasing trend is due to the limited time coverage (about 2.5 years), and the signal may be due to year-to-year variability. More data need to be collected to investigate the trend of CO on Reunion Island. Figure 5 shows that the seasonal cycles of CO from the in situ and FTIR measurements are very similar with the maximum in September–November and the minimum in February–April. The peak-to-peak amplitudes from NDACC and TCCON retrievals are very close ( $\sim 25$ – $28 \text{ ppb}$ ), and slightly weaker than that from the in situ measurements ( $\sim 32 \text{ ppb}$ ). The high value corresponds to the period when the island is downwind of emissions coming from biomass burning in Africa and South America (Duflot et al., 2010; Vigouroux et al., 2012).

The time series and the correlation between the colocated in situ and NDACC daily means of CO measurements at Maïdo are shown in Fig. 6. There are 448 data pairs. The daily standard deviation of the in situ measurements is larger than that of the NDACC retrievals. The difference (mean and standard deviation) between NDACC retrieved  $X_{\text{CO}}$  and in situ CO is  $15.69 \pm 10.02 \text{ ppb}$ , which is beyond the systematic uncertainty of the NDACC retrievals (2–3 ppb). The correlation coefficient ( $R$ ) between the NDACC and in situ measurements is 0.76. The slope ( $< 1.0$ ) indicates that the absolute difference between the in situ and NDACC measurements is large (small) for the low (high) CO values.

### 3.3 CH<sub>4</sub>

A clear positive trend for CH<sub>4</sub> is recognized in Fig. 4. The CH<sub>4</sub> annual growth is  $7.6 \pm 0.4 \text{ ppb yr}^{-1}$  for the TCCON measurements for 2011–2017, and  $7.4 \pm 0.5 \text{ ppb yr}^{-1}$  for the in situ measurements for the same time period at St Denis. Both estimations (at the surface and through the column) of the annual growth rates are in agreement with CH<sub>4</sub>

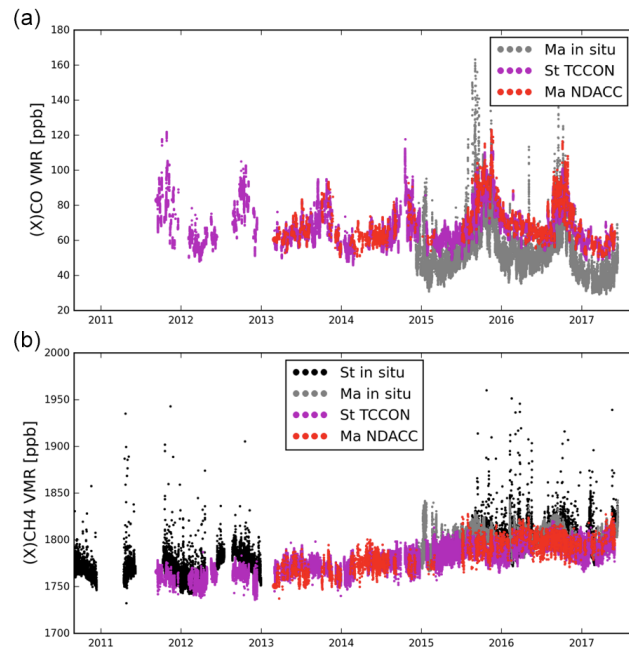


**Figure 4.** The time series of CO (a) and CH<sub>4</sub> (b) from in situ and FTIR (NDACC and TCCON) measurements at St Denis and Maïdo. Note that there is no CO in situ measurement at St Denis. “St” and “Ma” in the legend represent St Denis and Maïdo, respectively. “(X)gas” is used in the y axes labels to present in situ VMR measurements and FTIR  $X_{\text{gas}}$  retrievals together.

trends observed at other locations after 2007 (Rigby et al., 2008; Bader et al., 2017). Although there is also a positive trend ( $\sim 5.4 \text{ ppb yr}^{-1}$ ) for the TCCON a priori CH<sub>4</sub>, it has a weak effect on the trend of retrieved CH<sub>4</sub> since TCCON has a good sensitivity to the atmosphere, especially in the troposphere (see Fig. 2). The CH<sub>4</sub> annual growth is  $9.2 \pm 0.8 \text{ ppb yr}^{-1}$  from the NDACC retrievals from 2013 to 2017, and the annual growth of the TCCON measurements is  $7.9 \pm 0.4 \text{ ppb yr}^{-1}$  for the same time period. The annual growth of CH<sub>4</sub> in the 2013–2017 period is slightly larger than that in the 2011–2017 period, which is consistent with the results from the NOAA/ESRL cooperative global air sampling network ([https://www.esrl.noaa.gov/gmd/ccgg/trends\\_ch4/](https://www.esrl.noaa.gov/gmd/ccgg/trends_ch4/), last access: 23 September 2018). The globally averaged marine surface CH<sub>4</sub> annual increases from the NOAA/ESRL sites are  $7.7 \pm 0.6 \text{ ppb yr}^{-1}$  in the 2011–2017 period and  $8.8 \pm 0.7 \text{ ppb yr}^{-1}$  in the 2013–2017 period.

The seasonal cycles of CH<sub>4</sub> from the in situ measurements at St Denis and Maïdo are very close to the minimum in December–February and the maximum in August–September (see Fig. 5). This corresponds to the seasonal variation of OH radicals, which are the major sink of CH<sub>4</sub> in the atmosphere (Kirschke et al., 2013). The seasonal cycles from the NDACC and TCCON retrievals are also similar, but different from those of the in situ measurements. Both

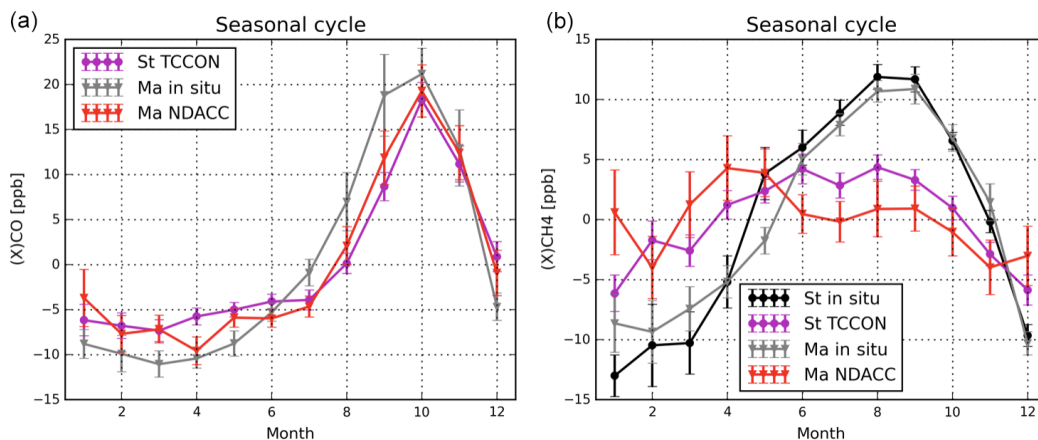


**Figure 5.** The seasonal cycles of CO (a) and CH<sub>4</sub> (b) from in situ and FTIR (NDACC and TCCON) measurements at St Denis and Maïdo. The error bar is  $1\sigma$  for all of the detrended data within that month.

NDACC and TCCON  $X_{\text{CH}_4}$  retrievals show high values in April–September and low values in October–March, but the seasonal cycle of  $X_{\text{CH}_4}$  from NDACC retrievals has a small peak in the March–May period. The amplitude of the seasonal cycle from the in situ measurements (about  $\pm 10$  ppb) is about 2 times larger than that from the FTIR measurements (about  $\pm 5$  ppb). The reasons for the different seasonal patterns between FTIR and in situ measurements are discussed in Sect. 4.

The time series and the correlation between the colocated in situ and TCCON daily means of CH<sub>4</sub> measurements at St Denis are shown in Fig. 7. The mean and standard deviation of the differences between the in situ and TCCON measurements are  $-6.63$  and  $9.78$  ppb, respectively. The standard deviation of  $9.78$  ppb is almost within the combination of the random uncertainties of the TCCON retrievals ( $\sim 9$  ppb) and of the in situ measurements ( $\sim 1$  ppb). Since there are no systematic uncertainties for both datasets, the mean value of  $-6.63$  ppb is the difference between CH<sub>4</sub> VMR at surface and the total column averaged CH<sub>4</sub> at St Denis. As there is a distinct positive annual growth for CH<sub>4</sub> for the 2011–2017 period, the correlation plot is labeled with the measurement year. The  $R$  between the TCCON  $X_{\text{CH}_4}$  and in situ CH<sub>4</sub> measurements is 0.86 for all of the data pairs. However, if we only take the data pairs after 2015, the  $R$  value drops to 0.48.

The time series and the correlation between the colocated in situ and NDACC daily means at Maïdo are shown in Fig. 8. The averaged daily standard deviation of NDACC retrievals is larger than that of in situ measurements, which is mainly due to the larger random error of NDACC retrievals (see Table 1). The mean and standard deviation of the differences between the in situ and FTIR measurements are 0.62 and 11.90 ppb, respectively. The difference also shows a distinct seasonal variation. The  $R$  value between daily NDACC  $X_{\text{CH}_4}$  and in situ surface CH<sub>4</sub> measurements is only 0.23. The lower correlation value is believed to be caused by the

limited number of colocated measurements ( $\sim 2$  years), and by the fact that NDACC CH<sub>4</sub> has a reduced sensitivity to the boundary layer and an increased sensitivity to the stratosphere compared to the CO product.

## 4 Discussions

### 4.1 CO

Atmospheric CO is mainly produced by the incomplete combustion of carbon-based fuels (Kasischke and Bruhwiler, 2002) and the oxidation of methane or other carbon-containing compounds (Cullis and Willatt, 1983). Maïdo observatory, being located on a remote mountain, has low anthropogenic CO emission nearby (European Commission, 2011); thus, there are very few spikes observed in the in situ measurements at this site in non-biomass-burning seasons (see upper panel in Figs. 4 and 6). Therefore, the CO molecules above Maïdo are either generated from oxidation processes in the atmosphere or transported from other places. FLEXible PARTicle dispersion model (FLEXPART) v9.02 (Stohl et al., 2005) backward simulations (see Fig. A1) are employed to understand the sources of air on Reunion Island. The settings of the FLEXPART run in this study are described in Appendix A. The results are consistent with Fig. 8 in Duflot et al. (2010). The air near the surface above Reunion Island mainly comes from the Indian Ocean and partly from southern Africa, whilst the air mass in the middle and upper troposphere mainly comes from Africa and South America. As CO emission on land is much larger than that from the ocean, FTIR  $X_{\text{CO}}$  is systematically larger than the in situ CO at the surface.

As we mentioned in Sect. 2.3.2, the NDACC retrievals provide CO profiles, which are comprised of approximately two individual layers of information (left panel in Fig. 3). We calculate the dry-air partial column averaged mole fractions

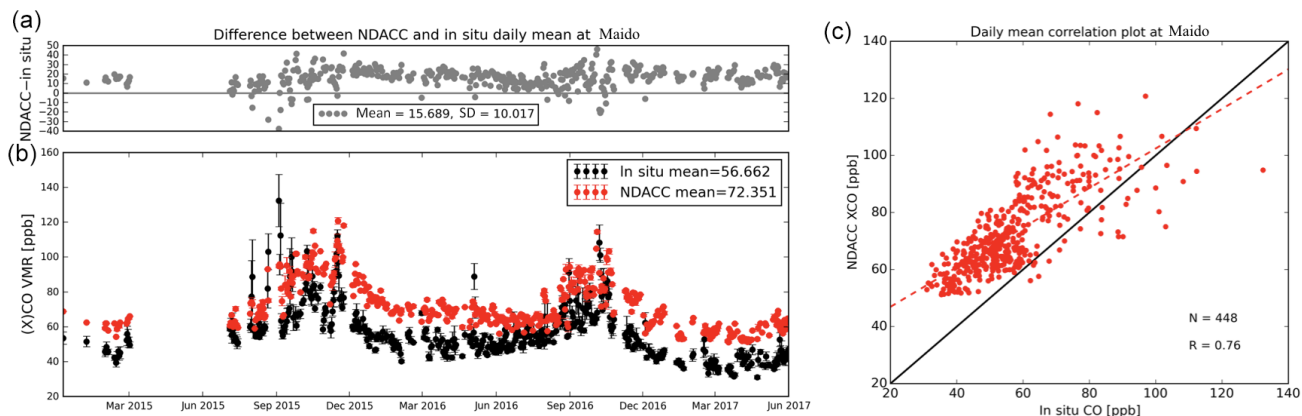


**Figure 6.** The time series of the daily means and standard deviations from FTIR (NDACC)  $X_{\text{CO}}$  and daytime in situ CO measurements at Maïdo, in addition to the absolute difference (unit: ppb) between them (left lower and top, respectively) and their correlation (right).

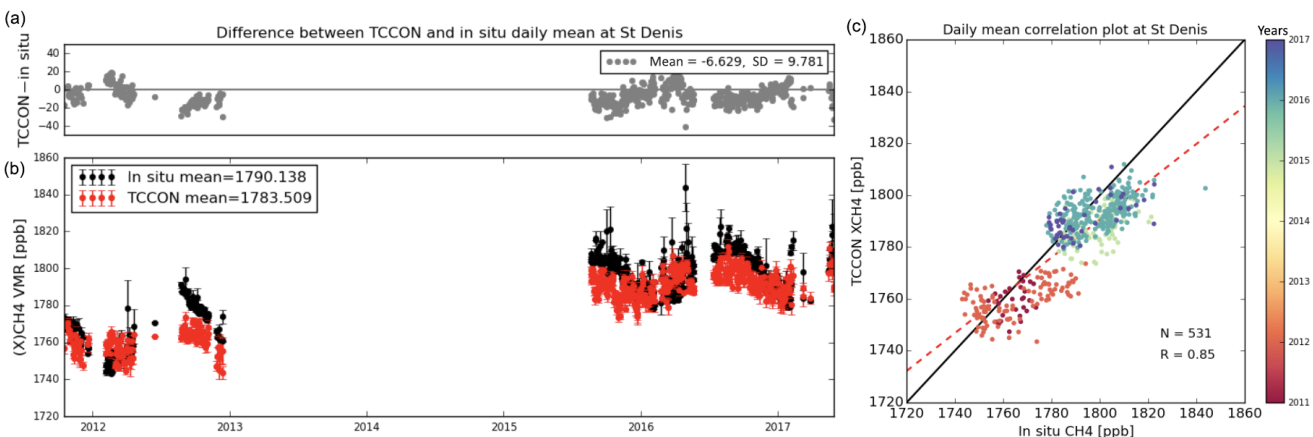


**Figure 7.** The time series of the daily means and standard deviations from the daytime in situ and FTIR (TCCON) CH<sub>4</sub> measurements at St Denis, in addition to the absolute difference (unit: ppb) between them (left lower and top, respectively) and their correlation (right). Since there is a distinct annual growth for CH<sub>4</sub>, the dots are colored according to the measurement year in the right panel.

$X_{\text{CO},p}$  in the vertical ranges of surface–8 km and 8–20 km following Eq. (5):

$$X_{\text{CO},p} = \text{PC}_{\text{CO},p}/\text{PC}_{\text{air},p}^{\text{dry}} = \text{PC}_{\text{CO},p}/(\text{PC}_{\text{air},p}^{\text{wet}} - \text{PC}_{\text{H}_2\text{O},p}), \quad (5)$$

where  $\text{PC}_{\text{CO},p}$ ,  $\text{PC}_{\text{H}_2\text{O},p}$ ,  $\text{PC}_{\text{air},p}^{\text{dry}}$  and  $\text{PC}_{\text{air},p}^{\text{wet}}$  are the partial column of CO, H<sub>2</sub>O, dry air and wet air in that vertical range.

The in situ CO measurements are compared with the NDACC  $X_{\text{CO},p}$  in the vertical range of surface–8 km and 8–20 km in Fig. 9. As we expected, the R value between the in situ and NDACC  $X_{\text{CO},p}$  in surface–8 km (0.81) is larger than the value between the in situ and NDACC  $X_{\text{CO},p}$  in 8–20 km (0.50). The large R value and the slope close to 1.0 between the in situ and NDACC  $X_{\text{CO},p}$  in surface–8 km confirm that NDACC CO retrievals have a very good sensitivity to the lower troposphere. NDACC retrievals show that air in the upper troposphere and the lower stratosphere also captures the signal from biomass burning despite the weaker peak. In

general, the peaks of CO at the surface, in the surface–8 km and the 8–20 km ranges, all occur in September–November, which are months that are dominated by biomass burning emissions.

## 4.2 CH<sub>4</sub>

### 4.2.1 Different seasonal cycles in the troposphere and stratosphere

In Sect. 3.3, we found that the seasonal cycles of CH<sub>4</sub> from the in situ and FTIR measurements are different. Ostler et al. (2016) pointed out that stratospheric CH<sub>4</sub> has an important contribution to the variation of the total column. Since the NDACC CH<sub>4</sub> retrievals have the ability to obtain two individual collections of information in the troposphere and the stratosphere, in this section, we separate the total column into tropospheric and stratospheric parts. Figure 10 shows

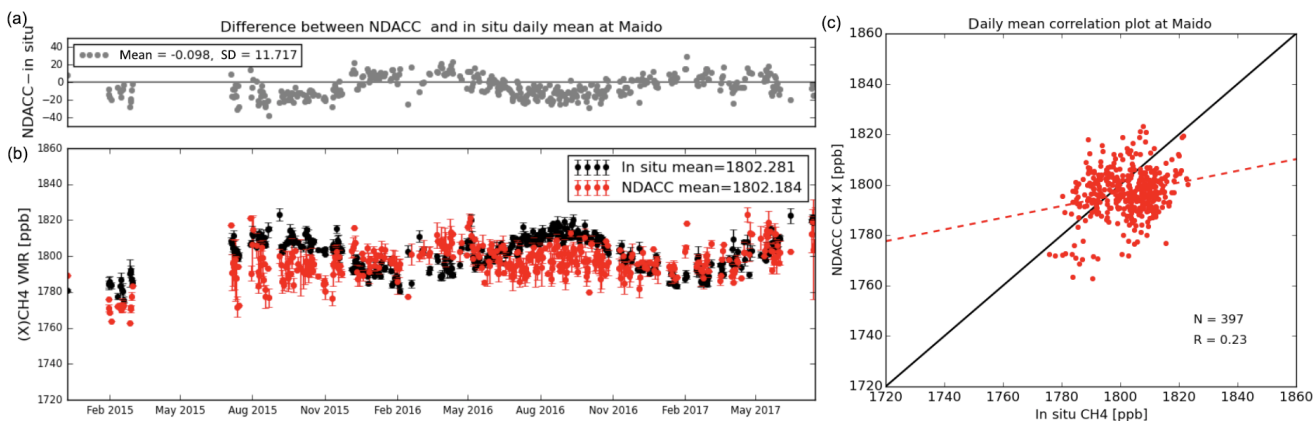


**Figure 8.** The time series of the daily means and standard deviations from the daytime in situ and FTIR (NDACC) CH<sub>4</sub> measurements at Maïdo, in addition to the absolute difference (unit: ppb) between them (a and b, respectively) and their correlation (c).

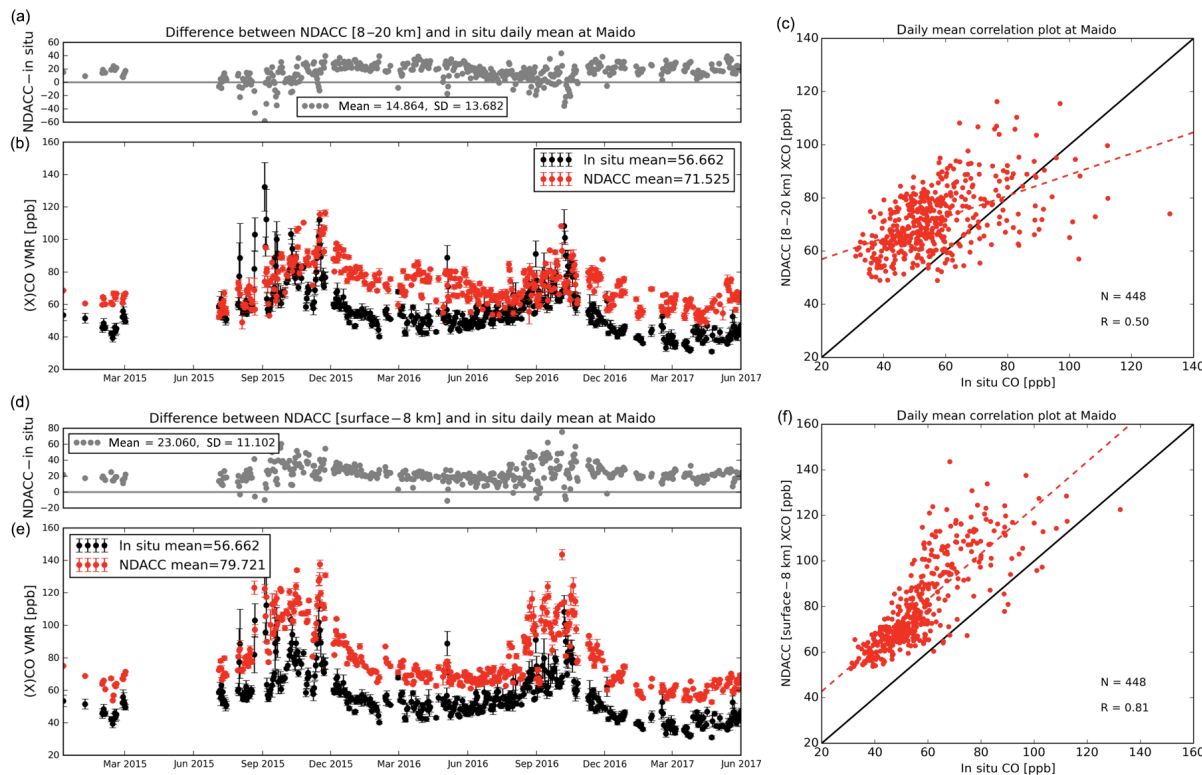


**Figure 9.** The time series of the daily means and standard deviations from the daytime in situ CO measurements and NDACC X<sub>CO</sub> in vertical ranges from 8 to 20 km (b) and the surface to 8 km (e) at Maïdo, in addition to the absolute difference (unit: ppb) between them (a, d) and their correlation (c, f).

the tropopause height above Reunion Island from the NCEP reanalysis data from 2000 to 2016. The tropopause height is about 16–17 km with the maximum in February–April and the minimum in August–October. The in situ measurements are treated as a reference to compare with the FTIR retrievals in the troposphere.

For NDACC retrieved CH<sub>4</sub> profiles, similar to X<sub>CO,p</sub> (Eq. 5), we calculate the dry-air column averaged mole fractions of CH<sub>4</sub> in the troposphere (X<sub>CH<sub>4</sub>,tr</sub>) and stratosphere

( $X_{\text{CH}_4,\text{st}}$ ), respectively:

$$\begin{aligned} X_{\text{CH}_4,\text{tr}} &= \text{PC}_{\text{CH}_4,\text{tr}}/\text{PC}_{\text{air},\text{tr}}^{\text{dry}} \\ &= \text{PC}_{\text{CH}_4,\text{tr}}/(\text{PC}_{\text{air},\text{tr}}^{\text{wet}} - \text{PC}_{\text{H}_2\text{O},\text{tr}}), \end{aligned} \quad (6)$$

$$X_{\text{CH}_4,\text{st}} = \text{PC}_{\text{CH}_4,\text{st}}/\text{PC}_{\text{air},\text{st}}^{\text{dry}}, \quad (7)$$

where  $\text{PC}_{\text{CH}_4,\text{tr}}$ ,  $\text{PC}_{\text{H}_2\text{O},\text{tr}}$ ,  $\text{PC}_{\text{air},\text{tr}}^{\text{dry}}$  and  $\text{PC}_{\text{air},\text{tr}}^{\text{wet}}$  are the respective partial columns of CH<sub>4</sub>, H<sub>2</sub>O, dry air and wet air in the troposphere;  $\text{PC}_{\text{CH}_4,\text{st}}$  and  $\text{PC}_{\text{air},\text{st}}^{\text{dry}}$  are the respective partial columns of CH<sub>4</sub> and dry air in the stratosphere. Note that the H<sub>2</sub>O partial column in the stratosphere is ignored as the H<sub>2</sub>O mole fraction is very low at high altitudes. We take the vertical range from the surface to 16.5 km as the troposphere and from 16.5 to 60 km as the stratosphere above Reunion Island.

For TCCON  $X_{\text{CH}_4}$  retrievals, it is not straightforward to separate the total column into tropospheric and stratospheric parts, as GGG2014 uses the scaling profile retrieval method. Fortunately, previous studies have proved that the HF total column (Washenfelder et al., 2003) or the stratospheric N<sub>2</sub>O (Wang et al., 2014) could be used as an estimator of the tropospheric CH<sub>4</sub>, since there is a good relationship between the CH<sub>4</sub> and HF or N<sub>2</sub>O in the stratosphere. The HF and N<sub>2</sub>O total columns are also retrieved from the TCCON spectra by GGG2014. However, the retrieved HF is seriously affected by the H<sub>2</sub>O mole fraction, especially at humid sites such as St Denis. Therefore, we use the N<sub>2</sub>O column to calculate the stratospheric CH<sub>4</sub> and the tropospheric CH<sub>4</sub>. The relationship between the stratospheric CH<sub>4</sub> and N<sub>2</sub>O is derived from the Atmospheric Chemistry Experiment Fourier transform spectrometer satellite data. For a thorough description of the N<sub>2</sub>O proxy method, refer to Wang et al. (2014).

In the stratosphere, the MIPAS satellite observations are applied to compare with the FTIR retrievals ( $X_{\text{CH}_4,\text{st}}$ ). MIPAS observed the global distributions of CH<sub>4</sub> profiles for the 2002–2012 period using the limb sounding technique. MIPAS performed in full spectral resolution mode (FR) with a spectral resolution of 0.05 cm<sup>-1</sup> from July 2002 to March 2004. After that, one of the interferometer sides was broken, and MIPAS switched to reduced spectral resolution mode (RR) with a spectral resolution of 0.121 cm<sup>-1</sup> (Fischer et al., 2008). In this section, we use the MIPAS level-2 version V5H (FR) and V5R (RR) data from the Institut für Meteorologie und Klimaforschung/Instituto de Astrofísica de Andalucía (von Clarmann et al., 2003). The MIPAS CH<sub>4</sub> profile covers the upper troposphere and the whole stratosphere (about 12–70 km). The DOFs of the CH<sub>4</sub> profile retrieved from MIPAS measurements is about 12 with a vertical resolution of 3–5 km below 50 km and 6–10 km above 50 km. The MIPAS observations in the vertical range of 16.5–60 km around Reunion Island within  $\pm 3^\circ$  latitude and  $\pm 5^\circ$  longitude are selected for comparison with the FTIR retrievals in the same vertical range. MIPAS observations show that the CH<sub>4</sub> mole fraction decreases with increasing altitude in the stratosphere.

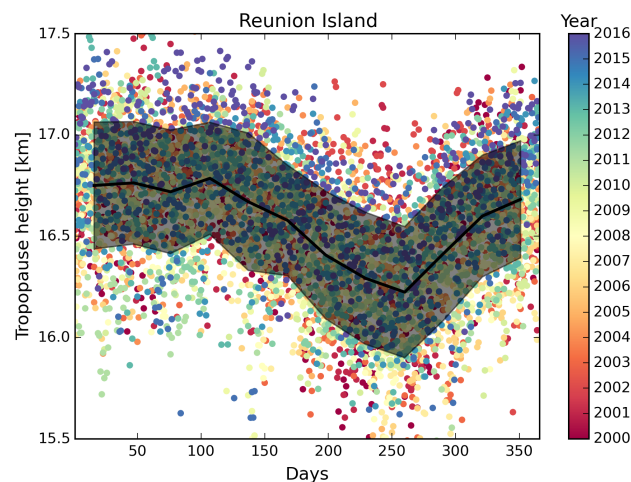


**Figure 10.** The tropopause height monthly means along with their uncertainties (shadow,  $1\sigma$ ) from the NCEP reanalysis data for the 2000–2016 period above Reunion Island.

The NDACC retrievals at St Denis for the 2004–2011 period are also analyzed in this section, because the MIPAS instrument stopped in April 2012. According to Rodgers (2003), the vertical sensitivity should be taken into account when comparing two remote sensing retrievals. As the vertical resolution of MIPAS observation is higher than that of FTIR measurement, a smoothing correction was carried out for the MIPAS profiles:

$$\text{PC}'_{\text{M}} = \text{PC}_{\text{a,N}} + \mathbf{A}(\mathbf{P}_{\text{M}} - \mathbf{P}_{\text{a,N}}), \quad (8)$$

where  $\mathbf{P}_{\text{a,N}}$  and  $\mathbf{P}_{\text{M}}$  are the NDACC a priori partial column profile and MIPAS retrieved partial column profile, respectively;  $\text{PC}_{\text{a,N}}$  is the NDACC a priori partial column (16.5–60 km);  $\text{PC}'_{\text{M}}$  is the smoothed MIPAS retrieved partial column (16.5–60 km); and  $\mathbf{A}$  is the partial column (16.5–60 km) averaging kernel of NDACC retrieval at St Denis. The  $X_{\text{CH}_4,\text{st}}$  from the MIPAS measurements are calculated to quantitatively compare with the FTIR retrievals, using Eq. (7).

Figure 11 shows the time series and seasonal cycles of CH<sub>4</sub> in the troposphere and stratosphere from the in situ, FTIR (NDACC and TCCON) and MIPAS (with and without smoothing correction) measurements. In the stratosphere, the difference between NDACC and TCCON retrievals is less than 0.5 %, which is within their measurement uncertainties. The MIPAS observations are slightly larger (about 30 ppb) compared to the NDACC measurements. The difference between MIPAS and NDACC measurements is within their error budget, as the averaged measurement uncertainty of MIPAS partial columns in the vertical range from 16.5 to 60 km is 3.5 % ( $\sim 50$  ppb). The seasonal cycles of stratospheric CH<sub>4</sub> from all measurements show a maximum in March–April and a minimum in August–October. Since CH<sub>4</sub> has a strong gradient near the tropopause, the seasonality is indica-

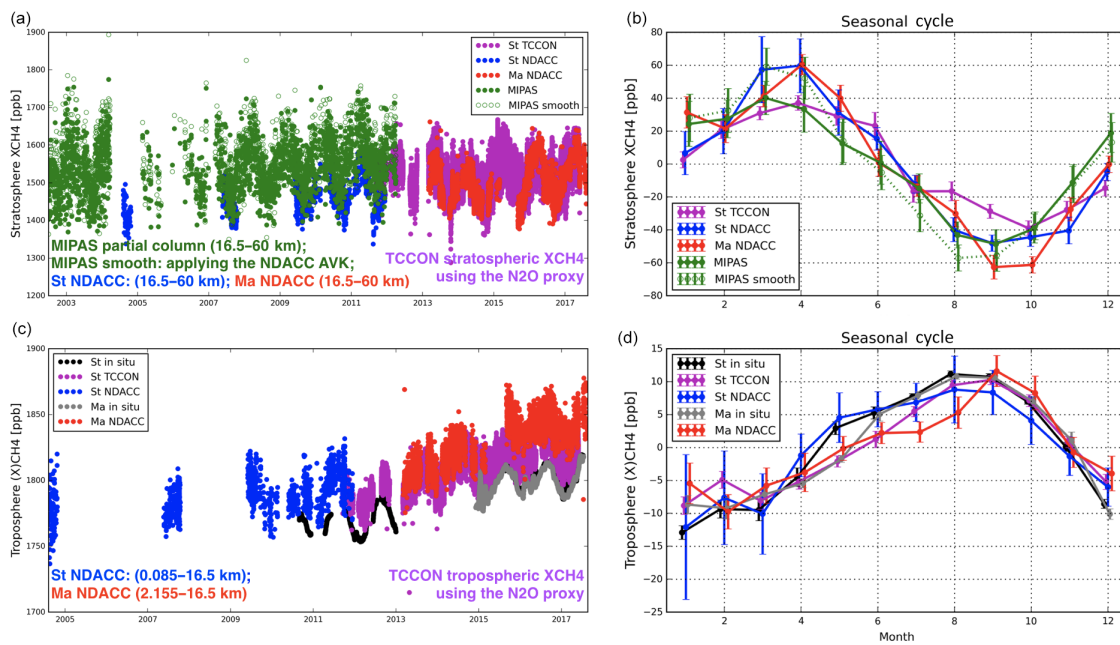


**Figure 11.** The time series and seasonal cycles of CH<sub>4</sub> from the in situ, FTIR (NDACC and TCCON) and colocated MIPAS measurements. (a) The time series of the stratospheric  $X_{\text{CH}_4}$  from the TCCON retrievals (the N<sub>2</sub>O proxy method) at St Denis, NDACC and colocated MIPAS partial columns (16.5–60 km), and the smoothed MIPAS measurements using the St Denis NDACC AVK. (b) The seasonal cycles of all the data in the stratosphere. (c) The time series of the tropospheric ( $X$ )CH<sub>4</sub> from the in situ measurements at St Denis and Maïdo, NDACC retrievals at St Denis (0.085–16.5 km) and Maïdo (2.155–16.5 km), and TCCON retrievals (the N<sub>2</sub>O proxy method) at St Denis. (d) The seasonal cycles of the available data in the troposphere.

tive of stratosphere–troposphere exchange and circulation in the near tropopause region (Park et al., 2004a). The pattern of the stratospheric  $X_{\text{CH}_4,\text{st}}$  seasonal cycle is highly related to the tropopause height (see Fig. 10), and the tropopause height is dominated by vertical transport (Holton et al., 1995). The enhanced CH<sub>4</sub> mole fraction during the March–April period could be due to convection, which lifts air from the troposphere to the stratosphere. The minimum in the August–October period comes from the strengthened sink down in the stratosphere. In August–October the upwelling branch of the Brewer–Dobson circulation moves to the Northern Hemisphere and the sink down motion occurs in the stratosphere above Reunion (Seviour et al., 2012). The amplitudes of the seasonal cycles from the TCCON and MIPAS measurements are about  $\pm 40$  ppb, which are lower than those derived from NDACC measurements (about  $\pm 60$  ppb). The AVK (the red line in the right panel of Fig. 3) shows that the retrieved partial column in the stratosphere from the NDACC retrieval overestimates the change in the stratosphere (AVK is about 1.3). After the smoothing correction, the amplitude of the seasonal cycle from the MIPAS measurements comes very close to the amplitudes from the NDACC retrievals at the two sites.

In the troposphere, the seasonal cycles of CH<sub>4</sub> from the in situ and the FTIR (both NDACC and TCCON) measurements have the same pattern with the maximum in August–

September and minimum in December–January, which is highly related to the OH seasonal variation (Bloss et al., 2005). In addition, all the amplitudes of the seasonal cycles are about  $\pm 10$  ppb. The CH<sub>4</sub> mole fraction from the in situ measurements at St Denis and Maïdo are very close. However, the in situ measurement is about 17 ppb lower than the TCCON  $X_{\text{CH}_4,\text{tr}}$  and about 27 ppb lower than the NDACC  $X_{\text{CH}_4,\text{tr}}$  on average. In the next section, the simulations from the GEOS-Chem model are used to understand the difference observed in absolute levels between the in situ, NDACC and TCCON CH<sub>4</sub> measurements in the troposphere.

#### 4.2.2 GEOS-Chem model simulations in the troposphere

The 3-D chemistry transport model GEOS-Chem (Wecht et al., 2014) is applied to investigate the seasonal cycle of methane in the troposphere and the differences between the in situ and the FTIR measurements of tropospheric CH<sub>4</sub>. This model is able to simulate the global vertical distributions of trace gases and aerosols. The methane offline simulation is performed with GEOS-Chem version 11-01, driven here by MERRA-2 reanalysis meteorological fields produced by the Global Modeling and Assimilation Office (GMAO) at the Goddard Space Flight Center. OH fields are prescribed from a 3-D archive of monthly mean OH concentrations (Park et al., 2004b), and the methane loss is augmented by

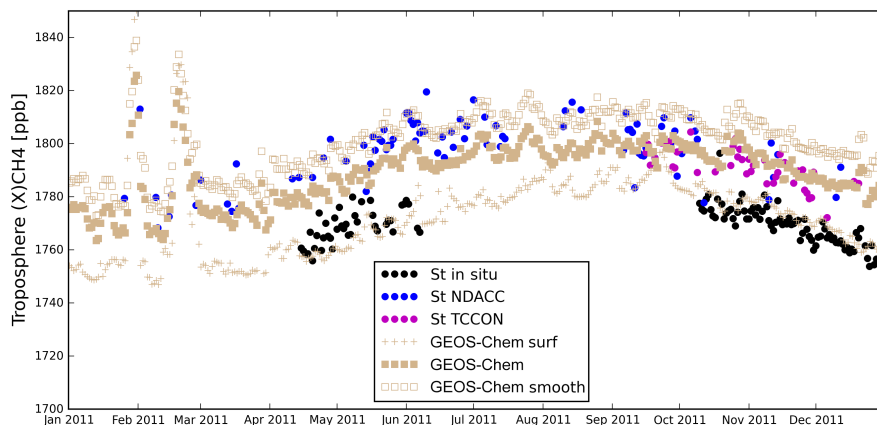


**Figure 12.** The time series of CH<sub>4</sub> daily means from the in situ measurements (black dots), NDACC tropospheric  $X_{\text{CH}_4}$  (blue dots) and TCCON tropospheric  $X_{\text{CH}_4}$  (purple dots) at St Denis, in addition to the GEOS-Chem model simulations of the VMR at the surface (brown cross), tropospheric  $X_{\text{CH}_4}$  (brown filled squares) and tropospheric  $X_{\text{CH}_4}$  after smoothing with NDACC AVK (brown empty squares) in 2011.

soil absorption (Fung et al., 1991). The methane emissions are computed at run time by the HEMCO module (Harvard-NASA Emission Component; Keller et al., 2014), notably accounting for the EDGAR v4.2 anthropogenic emissions inventory which includes oil and gas, coal mining, livestock, waste, residential biofuel emissions (European Commission, 2011) and the GFED4 biomass burning inventory (Randerson et al., 2015). We refer to Wecht et al. (2014) and Turner et al. (2015) for a description of the supplemental methane emission sources implemented in GEOS-Chem.

The whole year 2004 was used to spin-up the model simulation, adopting a  $2^\circ \times 2.5^\circ$  horizontal resolution and 47 levels, and merging the levels above about 80 hPa. The simulation was subsequently extended to cover the 2005–2011 time period. The GEOS-Chem outputs are saved every 3 hours, and a mass-conservative interpolation provides re-gridded methane profiles on the NDACC retrieval altitude scheme (see Sect. 3.1.1 in Bader et al., 2017). These GEOS-Chem profiles are eventually smoothed with the NDACC averaging kernels to ensure a fair comparison with the methane measurements (Rodgers, 2003).

Figure 12 compares the tropospheric measurements and the model results for the year 2011 at St Denis, the site and year for which all the measurement types are available. For the model simulation, surface CH<sub>4</sub> as well as the smoothed  $X_{\text{CH}_4}$  in the troposphere (using the NDACC tropospheric partial column averaging kernel in the 0.085–16.5 km altitude range) are compared with the in situ, NDACC and TCCON measurements, respectively. We did not apply the smoothing correction for model simulations with the TCCON AVK for the following two reasons: (1) TCCON only provides the AVK for the total column, and we are looking at the tropospheric partial column; and (2) using the TCCON total column AVK to correct the smoothing error in the vertical range from the surface to 16.5 km has also been tested,

and the averaged difference between the smoothed and unsmoothed model data is within 0.5 ppb. This difference is much smaller than that for the NDACC data, as the a priori profile of TCCON is very close to the model simulation.

The smoothed  $X_{\text{CH}_4}$  from GEOS-Chem is 11.5 ppb larger than the  $X_{\text{CH}_4}$  on average without smoothing. This is because the NDACC retrieved partial column in the troposphere is mostly sensitive to the vertical range of 5–13 km (see the blue line in the right panel of Fig. 3) and the modeled CH<sub>4</sub> mixing ratios are 15–30 ppb larger in this layer, when compared to surface mole fractions. As a result, the NDACC retrieved  $X_{\text{CH}_4}$  is larger than the TCCON retrievals in the troposphere. The GEOS-Chem simulation exhibits a clear seasonal modulation, with the maximum (minimum) mole fractions in August–September (December–January), which is primarily influenced by the OH variation throughout the year. This further indicates that the averaged CH<sub>4</sub> VMR at the surface is 16.7 ppb lower than the tropospheric  $X_{\text{CH}_4}$  (without smoothing), which is in good agreement with the in situ and TCCON measurements. To summarize, the model simulation captures the differences between in situ and FTIR measurements (both NDACC and TCCON) as well as the seasonal variation of methane in the troposphere. Apart from that, two obvious spikes of CH<sub>4</sub> were simulated by the GEOS-Chem model in January and February, and one was also observed by NDACC retrievals on 2 February 2011. The FLEXPART backward trajectories computed for this time period demonstrate that these spikes were due to the transport of air masses from the Northern Hemisphere to Reunion Island (see Fig. A2). Figure A1 also shows that air parcels over Reunion Island during the local summertime (December–February) partly come from the Northern Hemisphere, indicating that the Intertropical Convergence Zone (ITCZ) sometimes moves south over Reunion Island.

## 5 Conclusions

Atmospheric CO and CH<sub>4</sub> mole fractions are measured by the in situ and the FTIR instruments at two observatories (St Denis and Maïdo) on Reunion Island in the Indian Ocean. One Bruker IFS 125HR and one CRDS analyzer are currently operated at each site. The in situ measurements provide the CO and CH<sub>4</sub> VMR at the surface, while the FTIR techniques observe the abundance in the whole atmosphere along the solar light path. The FTIR at St Denis records NIR spectra, contributing to the TCCON network, while the FTIR at Maïdo records MIR spectra, contributing to the NDACC network.

The  $X_{\text{CO}}$  from the FTIR retrievals are compared with in situ measurements. The CO seasonal cycles observed from the in situ and NDACC and TCCON measurements are in good agreement with the maximum in September–November and the minimum in February–April. The CO maximum observed by both surface and total column measurements in the September–November period corresponds to the biomass burning period in Africa and South America. The NDACC CO retrievals have a strong sensitivity in the lower and middle troposphere, and a good correlation ( $R = 0.81$ ) is found between the colocated daily means from the in situ and NDACC partial column-averaged  $X_{\text{CO}}$  in the vertical range from the surface to 8 km. The averaged  $X_{\text{CO}}$  from NDACC retrievals is 15.7 ppb larger than the CO from in situ measurements at Maïdo. The different CO mole fraction between the surface and total column is related to the source of air on Reunion Island. FLEXPART simulations show that, during the entire year, the air near the surface mainly comes from the Indian Ocean and partly from southern Africa, while the air in the middle and upper troposphere is mainly from Africa and South America. The CO mole fraction from the ocean is much lower than that from the land. As a result, the  $X_{\text{CO}}$  from FTIR measurements at Maïdo is systematically about 15.7 ppb larger than the CO at the surface from in situ measurements.

The trend of CH<sub>4</sub> is  $7.6 \pm 0.4 \text{ ppb yr}^{-1}$  from the TCCON measurements for the 2011–2017 period, which is consistent with the trend of  $7.4 \pm 0.5 \text{ ppb yr}^{-1}$  from the in situ measurements for the same time period at St Denis. However, the seasonal cycles of CH<sub>4</sub> from the in situ and FTIR measurements are very different. The CH<sub>4</sub> mole fraction decreases rapidly with altitude above the tropopause height ( $\sim 16.5 \text{ km}$  on Reunion Island). According to the AVK, both NDACC and TCCON retrieved  $X_{\text{CH}_4}$  have a good sensitivity to the troposphere and stratosphere. The CH<sub>4</sub> seasonal cycles in the troposphere and stratosphere are analyzed separately, based on the in situ measurements, FTIR measurements and the colocated MIPAS satellite observations. A very good agreement is observed in the tropospheric and stratospheric CH<sub>4</sub> seasonal cycles between FTIR (NDACC and TCCON) measurements, and in situ and MIPAS measurements, respectively. In the troposphere, CH<sub>4</sub> VMR is high in August–September

and low in December–January, which is highly related to the OH seasonal variation. In the stratosphere, CH<sub>4</sub> mole fractions show a maximum in March–April and a minimum in August–October, which is dominated by vertical transport.

Finally, a simulation from the GEOS-Chem model is used to understand the differences observed in absolute levels between the in situ, NDACC and TCCON CH<sub>4</sub> measurements in the troposphere. The GEOS-Chem modeled CH<sub>4</sub> mixing ratios are 15–30 ppb larger in the middle and upper troposphere (4–16 km), when compared to surface mole fractions. As a result, GEOS-Chem  $X_{\text{CH}_4}$  in the troposphere is 16.7 ppb larger than the CH<sub>4</sub> at the surface, which is in line with the difference between the in situ and TCCON measurements. The difference between NDACC and TCCON retrieved  $X_{\text{CH}_4}$  is mainly due to the difference in vertical sensitivity. The averaged smoothed model simulation using the NDACC AVK is 11.5 ppb larger than the simulation without smoothing, which explains the difference between the NDACC and TCCON retrievals. In general, the in situ, NDACC and TCCON measurements are in good agreement with the GEOS-Chem model simulation.

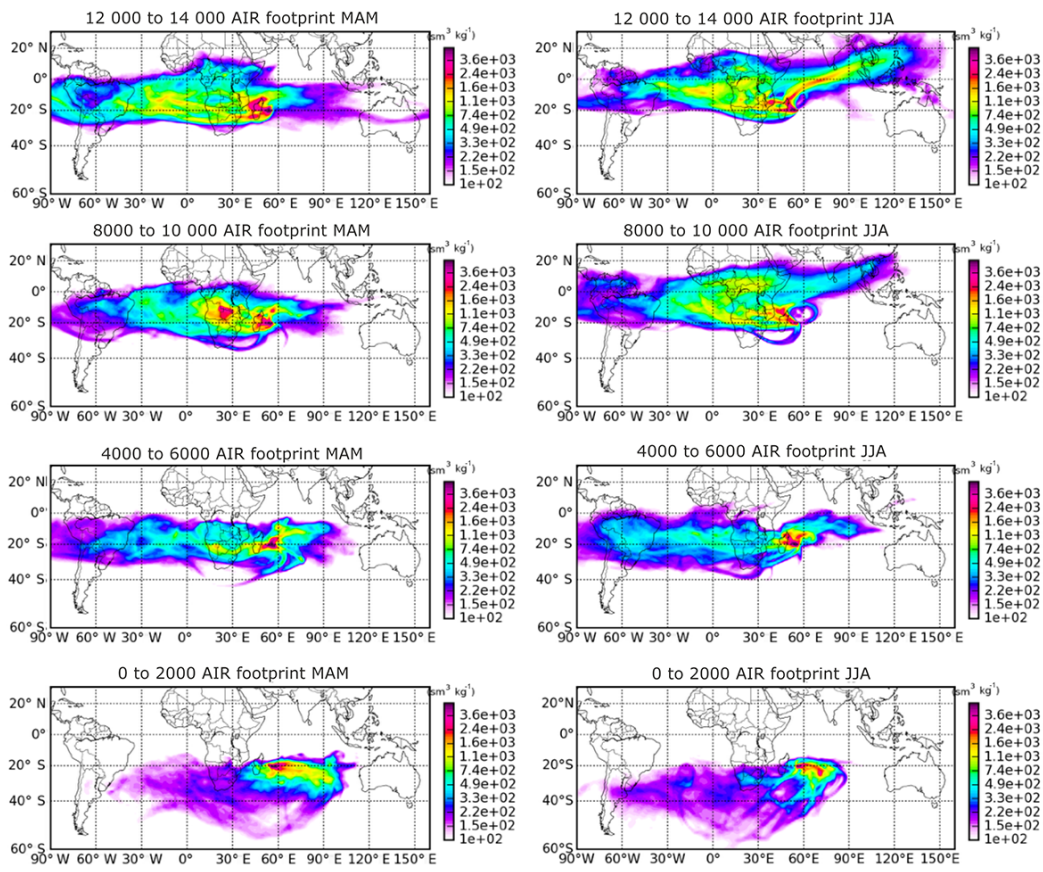
*Data availability.* The TCCON data at St Denis are publicly available through the TCCON wiki (<https://tccondata.org/>, last access: 25 September 2018). The NDACC data at St Denis and Maïdo are publicly available from the NDACC database (<ftp://ftp.cpc.ncep.noaa.gov/ndacc/>, last access: 25 September 2018). The in situ measurements from Reunion Island are not publicly available yet, but can be obtained by contacting the authors. The MIPAS satellite observations are publicly available from KIT/IMK (<https://www.imk-asf.kit.edu/english/308.php>, last access: 25 September 2018). The GEOS-Chem model data can be obtained from Emmanuel Mahieu ([emmanuel.mahieu@uliege.be](mailto:emmanuel.mahieu@uliege.be)).

## Appendix A: FLEXPART backward simulation

The Lagrangian particle dispersion model FLEXPART v9.02 is capable of simulating a large range of atmospheric transport processes, taking mean flow, deep convection, and turbulence into account (Stohl et al., 2005). The backward simulation of FLEXPART provides the release–receptor relationship, which is applied to study the source and transport of the observations from a measurement site. In this study, air particles are released over Reunion Island at four vertical ranges in the troposphere, and a 4-D response function (sensitivity) to emission inventory is calculated. The model was driven by the meteorological data from the European Centre for Medium-Range Weather Forecast (ECMWF). The residence time of particles in output grid cells describes the sensitivity of the receptor to the source. The detail settings of the FLEXPART backward run are listed in Table A1.

**Table A1.** The settings of FLEXPART v9.02 backward simulation used in this study.

Input meteorological data	ECMWF data at 1° × 1° global
Tracer	Air
Release location horizontal	±0.2° latitude/longitude around Reunion Island
Release location vertical	0–2000, 4000–6000, 8000–10000 and 12 000–14 000 m a.s.l.
Release time	06:00–18:00 local time for each day from 2011 to 2013
Number of days for backward running	20 days
Number of particles for each release	20 000
Output grid horizontal	1° × 1° global
Output grid vertical	0–16 000 m a.s.l.

**Figure A1.**

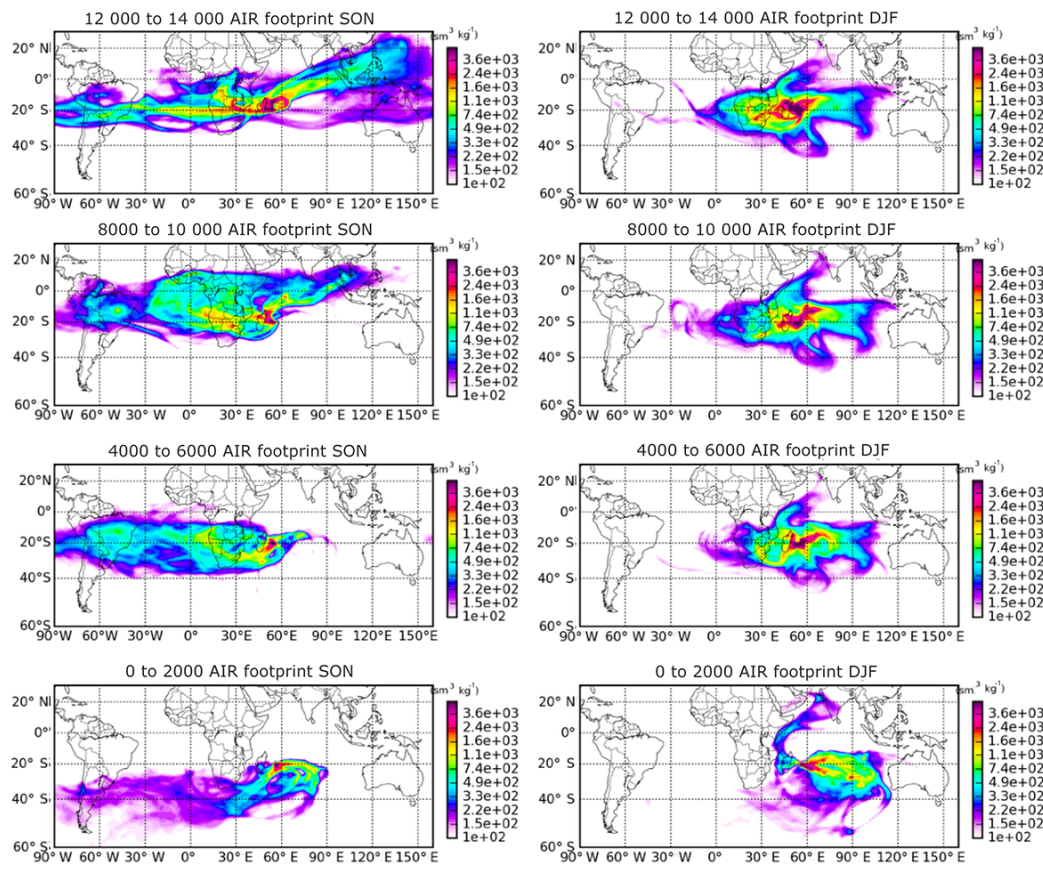


**Figure A1.** Seasonal distributions of the emission response sensitivity in backward simulations of the air at four vertical ranges (0–2000, 4000–6000, 8000–10 000 and 12 000–14 000 m a.s.l.) in the troposphere above Reunion Island in the 2011–2013 period simulated with FLEXPART v9.02 (20 day backward run). Sensitivity is given in units of  $\text{sm}^3 \text{ kg}^{-1}$ .

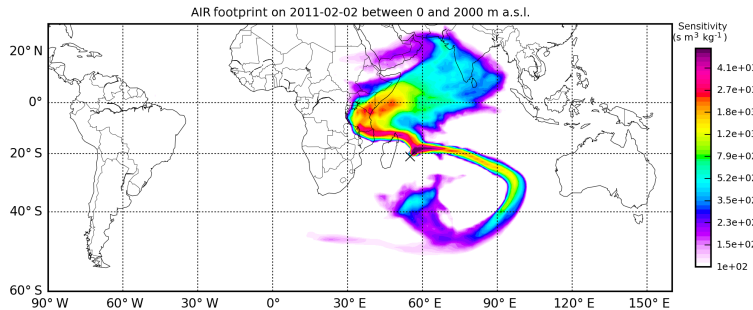


**Figure A2.** The emission response sensitivity of the air mass above Reunion Island in the vertical range from 0 to 2000 m a.s.l. on 2 February 2011 simulated with a 20 day backward run with FLEXPART v9.02.

**Author contributions.** MZ and MDM designed the study. MZ carried out the analysis. BL, CV, MKS and CH provided expertise on the FTIR data as well as the interpretation of the results. MR, MD, JMM, VD and NK provided and analysed the in situ measurements on Reunion Island. EM and WB provided the GEOS-Chem model simulation. ZW provided the TCCON tropospheric XCH<sub>4</sub> data. MP implemented the DLR H<sub>2</sub>O spectroscopy into the SFIT4 algorithm. MZ wrote the paper, with contributions from MR and EM.

**Competing interests.** The authors declare that they have no conflict of interest.

**Acknowledgements.** Harmonization and characterization of the NDACC and TCCON data were supported by the EU FP7 project QA4ECV and H2020 project GAIA-CLIM. Minqiang Zhou is supported by the Belgian Complementary Researchers program. The TCCON site at Reunion Island is operated by the Royal Belgian Institute for Space Aeronomy with financial support in 2014, 2015, 2016 and 2017 under the EU project ICOS-Inwire and the ministerial decree for ICOS (FR/35/IC2); local activities are supported by LACy/UMR8105, Université de La Réunion. The surface measurements are supported by the SNO RAMCES/ICOS-France. We would like to thank Evelyn De Watcher (BIRA-IASB) for helpful discussions, Bart Dils and Francis Scolas (BIRA-IASB) for their contribution to the FTIR measurements, and Cyrille Vuillemin, Delphine Combaz, Roxanne Jacob and Joyce Marais (LSCE) for their contribution to the in situ instrument maintenance. The authors also wish to thank the European Communities, the Région Réunion, CNRS and Université de la Réunion for their support and contribution in the construction phase of the research infrastructure OPAR. OPAR is presently funded by CNRS (INSU) and Université de La Réunion and managed by OSU-R (Observatoire des Sciences de l'Univers de La Réunion, UMS 3365). This work was supported by the German Research Foundation (DFG, project PA 1714/2-2). The MERRA-2 data used in this study were provided by the Global Modeling and Assimilation Office (GMAO) at NASA Goddard Space Flight Center. Whitney Bader received funding from the European Union's Horizon 2020 research and innovation programme under the Marie Skłodowska-Curie grant agreement no. 704951. The GEOS-Chem methane simulation at University of Liège was partly supported by the F.R.S.-FNRS (Brussels), under grant J.0093.15. Emmanuel Mahieu is a Research Associate with F.R.S.-FNRS.

Edited by: Andreas Richter

Reviewed by: two anonymous referees

## References

- Aschi, M. and Largo, A.: Reactivity of gaseous protonated ozone: A computational investigation on the carbon monoxide oxidation reaction, *Int. J. Mass Spectrom.*, 228, 613–627, [https://doi.org/10.1016/S1387-3806\(03\)00134-9](https://doi.org/10.1016/S1387-3806(03)00134-9), 2003.
- Bader, W., Bovy, B., Conway, S., Strong, K., Smale, D., Turner, A. J., Blumenstock, T., Boone, C., Collaud Coen, M., Coulon, A., Garcia, O., Griffith, D. W. T., Hase, F., Hausmann, P., Jones, N.,
- Krummel, P., Murata, I., Morino, I., Nakajima, H., O'Doherty, S., Paton-Walsh, C., Robinson, J., Sandrin, R., Schneider, M., Servais, C., Sussmann, R., and Mahieu, E.: The recent increase of atmospheric methane from 10 years of ground-based NDACC FTIR observations since 2005, *Atmos. Chem. Phys.*, 17, 2255–2277, <https://doi.org/10.5194/acp-17-2255-2017>, 2017.
- Baray, J.-L., Courcoux, Y., Keckhut, P., Portafaix, T., Tulet, P., Cammas, J.-P., Hauchecorne, A., Godin Beekmann, S., De Mazière, M., Hermans, C., Desmet, F., Sellegri, K., Colomb, A., Ramonet, M., Sciare, J., Vuillemin, C., Hoareau, C., Dionisi, D., Duflot, V., Vérèmes, H., Porteneuve, J., Gabarrot, F., Gaudio, T., Metzger, J.-M., Payen, G., Leclair de Bellevue, J., Barthe, C., Posny, F., Ricaud, P., Abchiche, A., and Delmas, R.: Maïdo observatory: a new high-altitude station facility at Reunion Island (21° S, 55° E) for long-term atmospheric remote sensing and in situ measurements, *Atmos. Meas. Tech.*, 6, 2865–2877, <https://doi.org/10.5194/amt-6-2865-2013>, 2013.
- Birk, M., Wagner, G., Loos, J., Lodi, L., Polyansky, O. L., Kyuberis, A. A., Zobov, N. F., and Tennyson, J.: Accurate line intensities for water transitions in the infrared: Comparison of theory and experiment, *J. Quant. Spectrosc. Ra.*, 203, 88–102, <https://doi.org/10.1016/J.JQSRT.2017.03.040>, 2017.
- Bloss, W. J., Evans, M. J., Lee, J. D., Sommariva, R., Heard, D. E., and Pilling, M. J.: The oxidative capacity of the troposphere: Coupling of field measurements of OH and a global chemistry transport model, *Faraday Discuss.*, 130, 425–436, <https://doi.org/10.1039/b419090d>, 2005.
- Cullis, C. F. and Willatt, B. M.: Oxidation of methane over supported precious metal catalysts, *J. Catal.*, 83, 267–285, [https://doi.org/10.1016/0021-9517\(83\)90054-4](https://doi.org/10.1016/0021-9517(83)90054-4), 1983.
- De Maziere, M., Sha, M. K., Desmet, F., Hermans, C., Scolas, F., Kumps, N., Metzger, J.-M., Duflot, V., and Cammas, J.-P.: TCCON data from Reunion Island (La Réunion), France, Release GGG2014R0. TCCON data archive, hosted by Caltech-DATA, California Institute of Technology, Pasadena, CA, USA, <https://doi.org/10.14291/tccn.ggg2014.reunion01.R0/1149288>, 2017.
- Deeter, M. N., Martínez-Alonso, S., Edwards, D. P., Emmons, L. K., Gille, J. C., Worden, H. M., Sweeney, C., Pittman, J. V., Daube, B. C., and Wofsy, S. C.: The MOPITT Version 6 product: algorithm enhancements and validation, *Atmos. Meas. Tech.*, 7, 3623–3632, <https://doi.org/10.5194/amt-7-3623-2014>, 2014.
- Dils, B., Cui, J., Henne, S., Mahieu, E., Steinbacher, M., and De Mazière, M.: 1997–2007 CO trend at the high Alpine site Jungfraujoch: a comparison between NDIR surface in situ and FTIR remote sensing observations, *Atmos. Chem. Phys.*, 11, 6735–6748, <https://doi.org/10.5194/acp-11-6735-2011>, 2011.
- Duflot, V., Dils, B., Baray, J. L., De Mazière, M., Attié, J. L., Vanhaevelyn, G., Senten, C., Vigouroux, C., Clain, G., and Delmas, R.: Analysis of the origin of the distribution of CO in the subtropical southern Indian Ocean in 2007, *J. Geophys. Res.-Atmos.*, 115, 1–16, <https://doi.org/10.1029/2010JD013994>, 2010.
- European Commission: Emission Database for Global Atmospheric Research (EDGAR), release version 4.2, Tech. rep., Joint Research Centre (JRC)/Netherlands Environmental Assessment Agency (PBL), <http://edgar.jrc.ec.europa.eu> (last access: 22 February 2018), 2011.
- Fischer, H., Birk, M., Blom, C., Carli, B., Carlotti, M., von Claramann, T., Delbouille, L., Dudhia, A., Ehnhalt, D., Endemann, M.,

- Flaud, J. M., Gessner, R., Kleinert, A., Koopman, R., Langen, J., López-Puertas, M., Mosner, P., Nett, H., Oelhaf, H., Perron, G., Remedios, J., Ridolfi, M., Stiller, G., and Zander, R.: MI-PAS: an instrument for atmospheric and climate research, *Atmos. Chem. Phys.*, 8, 2151–2188, <https://doi.org/10.5194/acp-8-2151-2008>, 2008.
- Folini, D., Kaufmann, P., Ubl, S., and Henne, S.: Region of influence of 13 remote European measurement sites based on modeled carbon monoxide mixing ratios, *J. Geophys. Res.-Atmos.*, 114, D08307, <https://doi.org/10.1029/2008JD011125>, 2009.
- Fung, I., John, J., Lerner, J., Matthews, E., Prather, M., Steele, L. P., and Fraser, P. J.: Three-dimensional model synthesis of the global methane cycle, *J. Geophys. Res.*, 96, 13033, <https://doi.org/10.1029/91JD01247>, 1991.
- Hazan, L., Tarniewicz, J., Ramonet, M., Laurent, O., and Abbaris, A.: Automatic processing of atmospheric CO<sub>2</sub> and CH<sub>4</sub> mole fractions at the ICOS Atmosphere Thematic Centre, *Atmos. Meas. Tech.*, 9, 4719–4736, <https://doi.org/10.5194/amt-9-4719-2016>, 2016.
- Holton, J. R., Haynes, P. H., McIntyre, M. E., Douglass, A. R., Rood, R. B., and Pfister, L.: Stratosphere-troposphere exchange, *Rev. Geophys.*, 33, 403–439, <https://doi.org/10.1029/95RG02097>, 1995.
- IPCC: Climate change 2013: The physical science basis, Contribution of Working Group I to the Fifth Assessment Report of the Intergovernmental Panel on Climate Change, 2013.
- Kasischke, E. S. and Bruhwiler, L. P.: Emissions of carbon dioxide, carbon monoxide, and methane from boreal forest fires in 1998, *J. Geophys. Res.-Atmos.*, 107, 8146, <https://doi.org/10.1029/2001JD000461>, 2002.
- Keller, C. A., Long, M. S., Yantosca, R. M., Da Silva, A. M., Pawson, S., and Jacob, D. J.: HEMCO v1.0: a versatile, ESMF-compliant component for calculating emissions in atmospheric models, *Geosci. Model Dev.*, 7, 1409–1417, <https://doi.org/10.5194/gmd-7-1409-2014>, 2014.
- Kiel, M., Hase, F., Blumenstock, T., and Kirner, O.: Comparison of XCO abundances from the Total Carbon Column Observing Network and the Network for the Detection of Atmospheric Composition Change measured in Karlsruhe, *Atmos. Meas. Tech.*, 9, 2223–2239, <https://doi.org/10.5194/amt-9-2223-2016>, 2016.
- Kirschke, S., Bousquet, P., Ciais, P., Saunois, M., Canadell, J. G., Drlugokencky, E. J., Bergamaschi, P., Bergmann, D., Blake, D. R., Bruhwiler, L., Cameron-Smith, P., Castaldi, S., Chevallier, F., Feng, L., Fraser, A., Heimann, M., Hodson, E. L., Houweling, S., Josse, B., Fraser, P. J., Krummel, P. B., Lamarque, J.-F., Langenfelds, R. L., Le Quéré, C., Naik, V., O'Doherty, S., Palmer, P. I., Pison, I., Plummer, D., Poulter, B., Prinn, R. G., Rigby, M., Ringeval, B., Santini, M., Schmidt, M., Shindell, D. T., Simpson, I. J., Spahni, R., Steele, L. P., Strode, S. A., Sudo, K., Szopa, S., van der Werf, G. R., Voulgarakis, A., van Weele, M., Weiss, R. F., Williams, J. E., and Zeng, G.: Three decades of global methane sources and sinks, *Nat. Geosci.*, 6, 813–823, <https://doi.org/10.1038/ngeo1955>, 2013.
- Laurent, O.: ICOS Atmospheric Station Specifications, [https://icos-atc.lsce.ipsl.fr/doc\\_public](https://icos-atc.lsce.ipsl.fr/doc_public) (last access: 28 September 2018), 2016.
- Loos, J., Birk, M., and Wagner, G.: Measurement of air-broadening line shape parameters and temperature dependence parameters of H<sub>2</sub>O lines in the spectral ranges 1850–2280 cm<sup>-1</sup> and 2390–4000 cm<sup>-1</sup>, *J. Quant. Spectrosc. Ra.*, 203, 103–118, <https://doi.org/10.1016/J.JQSRT.2017.03.033>, 2017a.
- Loos, J., Birk, M., and Wagner, G.: Measurement of positions, intensities and self-broadening line shape parameters of H<sub>2</sub>O lines in the spectral ranges 1850–2280 cm<sup>-1</sup> and 2390–4000 cm<sup>-1</sup>, *J. Quant. Spectrosc. Ra.*, 203, 119–132, <https://doi.org/10.1016/J.JQSRT.2017.02.013>, 2017b.
- Lopez, M., Schmidt, M., Ramonet, M., Bonne, J.-L., Colomb, A., Kazan, V., Laj, P., and Pichon, J.-M.: Three years of semi-continuous greenhouse gas measurements at the Puy de Dôme station (central France), *Atmos. Meas. Tech.*, 8, 3941–3958, <https://doi.org/10.5194/amt-8-3941-2015>, 2015.
- Messerschmidt, J., Geibel, M. C., Blumenstock, T., Chen, H., Deutscher, N. M., Engel, A., Feist, D. G., Gerbig, C., Gisi, M., Hase, F., Katrynski, K., Kolle, O., Lavric, J. V., Notholt, J., Palm, M., Ramonet, M., Rettinger, M., Schmidt, M., Sussmann, R., Toon, G. C., Truong, F., Warneke, T., Wennberg, P. O., Wunch, D., and Xueref-Remy, I.: Calibration of TCCON column-averaged CO<sub>2</sub>: the first aircraft campaign over European TCCON sites, *Atmos. Chem. Phys.*, 11, 10765–10777, <https://doi.org/10.5194/acp-11-10765-2011>, 2011.
- Novelli, P. C.: Reanalysis of tropospheric CO trends: Effects of the 1997–1998 wildfires, *J. Geophys. Res.*, 108, 4464, <https://doi.org/10.1029/2002JD003031>, 2003.
- Novelli, P. C., Masarie, K. A., and Lang, P. M.: Distributions and recent changes of carbon monoxide in the lower troposphere, *J. Geophys. Res.-Atmos.*, 103, 19015–19033, <https://doi.org/10.1029/98JD01366>, 1998.
- Ostler, A., Sussmann, R., Rettinger, M., Deutscher, N. M., Dohe, S., Hase, F., Jones, N., Palm, M., and Sinnhuber, B.-M.: Multistation intercomparison of column-averaged methane from NDACC and TCCON: impact of dynamical variability, *Atmos. Meas. Tech.*, 7, 4081–4101, <https://doi.org/10.5194/amt-7-4081-2014>, 2014.
- Ostler, A., Sussmann, R., Patra, P. K., Houweling, S., De Bruine, M., Stiller, G. P., Haenel, F. J., Plieninger, J., Bousquet, P., Yin, Y., Saunois, M., Walker, K. A., Deutscher, N. M., Griffith, D. W. T., Blumenstock, T., Hase, F., Warneke, T., Wang, Z., Kivi, R., and Robinson, J.: Evaluation of column-averaged methane in models and TCCON with a focus on the stratosphere, *Atmos. Meas. Tech.*, 9, 4843–4859, <https://doi.org/10.5194/amt-9-4843-2016>, 2016.
- Park, M., Randel, W. J., Kinnison, D. E., Garcia, R. R., and Choi, W.: Seasonal variation of methane, water vapor, and nitrogen oxides near the tropopause: Satellite observations and model simulations, *J. Geophys. Res.-Atmos.*, 109, D03302, <https://doi.org/10.1029/2003JD003706>, 2004a.
- Park, R. J., Jacob, D. J., Field, B. D., Yantosca, R. M., and Chin, M.: Natural and transboundary pollution influences on sulfate-nitrate-ammonium aerosols in the United States: Implications for policy, *J. Geophys. Res.-Atmos.*, 109, D15204, <https://doi.org/10.1029/2003JD004473>, 2004b.
- Pougatchev, N. S., Connor, B. J., and Rinsland, C. P.: Infrared measurements of the ozone vertical distribution above Kitt Peak, *J. Geophys. Res.*, 100, 16689, <https://doi.org/10.1029/95JD01296>, 1995.
- Randerson, J. T., van der Werf, G. R., Giglio, L., Collatz, G. J., and Kasibhatla, P. S.: Global Fire Emissions Database, Version 4, (GFEDv4), <https://doi.org/10.3334/ORNLDAC/1293>, 2015.

- Rasmussen, R. A. and Khalil, M. A. K.: Atmospheric methane (CH<sub>4</sub>): Trends and seasonal cycles, *J. Geophys. Res.-Oceans*, 86, 9826–9832, <https://doi.org/10.1029/JC086iC10p09826>, 1981.
- Rella, C. W., Chen, H., Andrews, A. E., Filges, A., Gerbig, C., Hatakka, J., Karion, A., Miles, N. L., Richardson, S. J., Steinbacher, M., Sweeney, C., Wastine, B., and Zellweger, C.: High accuracy measurements of dry mole fractions of carbon dioxide and methane in humid air, *Atmos. Meas. Tech.*, 6, 837–860, <https://doi.org/10.5194/amt-6-837-2013>, 2013.
- Rigby, M., Prinn, R. G., Fraser, P. J., Simmonds, P. G., Langenfelds, R. L., Huang, J., Cunnold, D. M., Steele, L. P., Krummel, P. B., Weiss, R. F., O'Doherty, S., Salameh, P. K., Wang, H. J., Harth, C. M., Mühle, J., and Porter, L. W.: Renewed growth of atmospheric methane, *Geophys. Res. Lett.*, 35, L22805, <https://doi.org/10.1029/2008GL036037>, 2008.
- Rodgers, C. D.: Inverse Methods for Atmospheric Sounding – Theory and Practice, Series on Atmospheric Oceanic and Planetary Physics, vol. 2, World Scientific Publishing Co. Pte. Ltd, Singapore, <https://doi.org/10.1142/9789812813718>, 2000.
- Rodgers, C. D.: Intercomparison of remote sounding instruments, *J. Geophys. Res.*, 108, 46–48, <https://doi.org/10.1029/2002JD002299>, 2003.
- Senten, C., De Mazière, M., Dils, B., Hermans, C., Kruglanski, M., Neefs, E., Scolas, F., Vandaele, A. C., Vanhaelewijn, G., Vigouroux, C., Carleer, M., Coheur, P. F., Fally, S., Barret, B., Baray, J. L., Delmas, R., Leveau, J., Metzger, J. M., Mahieu, E., Boone, C., Walker, K. A., Bernath, P. F., and Strong, K.: Technical Note: New ground-based FTIR measurements at Ile de La Réunion: observations, error analysis, and comparisons with independent data, *Atmos. Chem. Phys.*, 8, 3483–3508, <https://doi.org/10.5194/acp-8-3483-2008>, 2008.
- Sepúlveda, E., Schneider, M., Hase, F., Barthlott, S., Dubravica, D., García, O. E., Gomez-Pelaez, A., González, Y., Guerra, J. C., Gisi, M., Kohlhepp, R., Dohe, S., Blumenstock, T., Strong, K., Weaver, D., Palm, M., Sadeghi, A., Deutscher, N. M., Warneke, T., Notholt, J., Jones, N., Griffith, D. W. T., Smale, D., Brailsford, G. W., Robinson, J., Meinhardt, F., Steinbacher, M., Aalto, T., and Worthy, D.: Tropospheric CH<sub>4</sub> signals as observed by NDACC FTIR at globally distributed sites and comparison to GAW surface in situ measurements, *Atmos. Meas. Tech.*, 7, 2337–2360, <https://doi.org/10.5194/amt-7-2337-2014>, 2014.
- Seviour, W. J. M., Butchart, N., and Hardiman, S. C.: The Brewer-Dobson circulation inferred from ERA-Interim, *Q. J. R. Meteor. Soc.*, 138, 878–888, <https://doi.org/10.1002/qj.966>, 2012.
- Stohl, A., Forster, C., Frank, A., Seibert, P., and Wotawa, G.: Technical note: The Lagrangian particle dispersion model FLEXPART version 6.2, *Atmos. Chem. Phys.*, 5, 2461–2474, <https://doi.org/10.5194/acp-5-2461-2005>, 2005.
- Sussmann, R., Forster, F., Rettinger, M., and Bousquet, P.: Renewed methane increase for five years (2007–2011) observed by solar FTIR spectrometry, *Atmos. Chem. Phys.*, 12, 4885–4891, <https://doi.org/10.5194/acp-12-4885-2012>, 2012.
- Té, Y., Jeseck, P., Franco, B., Mahieu, E., Jones, N., Paton-Walsh, C., Griffith, D. W. T., Buchholz, R. R., Hadji-Lazaro, J., Hurtmans, D., and Janssen, C.: Seasonal variability of surface and column carbon monoxide over the megacity Paris, high-altitude Jungfraujoch and Southern Hemispheric Wolongong stations, *Atmos. Chem. Phys.*, 16, 10911–10925, <https://doi.org/10.5194/acp-16-10911-2016>, 2016.
- Toon, G. C.: Telluric line list for GGG2014, TCCON data archive, hosted by the Carbon Dioxide Information Analysis Center, Oak Ridge National Laboratory, Oak Ridge, Tennessee, USA, <https://doi.org/10.14291/tccon.ggg2014.atm.R0/1221656>, 2014.
- Toon, G. C. and Wunch, D.: A stand-alone a priori profile generation tool for GGG2014 release, TCCON data archive, hosted by the Carbon Dioxide Information Analysis Center, Oak Ridge National Laboratory, Oak Ridge, Tennessee, USA, <https://doi.org/10.14291/TCCON.GGG2014.PRIORS.R0/1221661>, 2014.
- Turner, A. J., Jacob, D. J., Wecht, K. J., Maasakkers, J. D., Lundgren, E., Andrews, A. E., Biraud, S. C., Boesch, H., Bowman, K. W., Deutscher, N. M., Dubey, M. K., Griffith, D. W. T., Hase, F., Kuze, A., Notholt, J., Ohyama, H., Parker, R., Payne, V. H., Sussmann, R., Sweeney, C., Velasco, V. A., Warneke, T., Wennberg, P. O., and Wunch, D.: Estimating global and North American methane emissions with high spatial resolution using GOSAT satellite data, *Atmos. Chem. Phys.*, 15, 7049–7069, <https://doi.org/10.5194/acp-15-7049-2015>, 2015.
- Vermeulen, A. T., Hensen, A., Popa, M. E., van den Bulk, W. C. M., and Jongejan, P. A. C.: Greenhouse gas observations from Cabauw Tall Tower (1992–2010), *Atmos. Meas. Tech.*, 4, 617–644, <https://doi.org/10.5194/amt-4-617-2011>, 2011.
- Vigouroux, C., Stavrakou, T., Whaley, C., Dils, B., Duflot, V., Hermans, C., Kumps, N., Metzger, J.-M., Scolas, F., Vanhaelewijn, G., Müller, J.-F., Jones, D. B. A., Li, Q., and De Mazière, M.: FTIR time-series of biomass burning products (HCN, C<sub>2</sub>H<sub>6</sub>, C<sub>2</sub>H<sub>2</sub>, CH<sub>3</sub>OH, and HCOOH) at Reunion Island (21° S, 55° E) and comparisons with model data, *Atmos. Chem. Phys.*, 12, 10367–10385, <https://doi.org/10.5194/acp-12-10367-2012>, 2012.
- von Clarmann, T., Ceccherini, S., Doicu, A., Dudhia, A., Funke, B., Grabowski, U., Hilgers, S., Jay, V., Linden, A., Lopez-Puertas, M., Martin-Torres, F. J., Payne, V., Reburn, J., Ridolfi, M., Schreier, F., Schwarz, G., Siddans, R., and Steck, T.: A blind test retrieval experiment for infrared limb emission spectrometry, *J. Geophys. Res.*, 108, 4746, <https://doi.org/10.1029/2003jd003835>, 2003.
- Wang, Z., Deutscher, N. M., Warneke, T., Notholt, J., Dils, B., Griffith, D. W. T., Schmidt, M., Ramonet, M., and Gerbig, C.: Retrieval of tropospheric column-averaged CH<sub>4</sub> mole fraction by solar absorption FTIR-spectrometry using N<sub>2</sub>O as a proxy, *Atmos. Meas. Tech.*, 7, 3295–3305, <https://doi.org/10.5194/amt-7-3295-2014>, 2014.
- Washenfelder, R. A., Wennberg, P. O., and Toon, G. C.: Tropospheric methane retrieved from ground-based near-IR solar absorption spectra, *Geophys. Res. Lett.*, 30, 2226, <https://doi.org/10.1029/2003GL017969>, 2003.
- Wecht, K. J., Jacob, D. J., Frankenberg, C., Jiang, Z., and Blake, D. R.: Mapping of North American methane emissions with high spatial resolution by inversion of SCIAMACHY satellite data, *J. Geophys. Res.*, 119, 7741–7756, <https://doi.org/10.1002/2014JD021551>, 2014.
- Wunch, D., Toon, G. C., Wennberg, P. O., Wofsy, S. C., Stephens, B. B., Fischer, M. L., Uchino, O., Abshire, J. B., Bernath, P., Biraud, S. C., Blavier, J.-F. L., Boone, C., Bowman, K. P., Brownell, E. V., Campos, T., Connor, B. J., Daube, B. C., Deutscher, N. M., Diao, M., Elkins, J. W., Gerbig, C., Gottlieb, E., Griffith, D. W. T., Hurst, D. F., Jiménez, R., Keppel-Aleks, G., Kort,

- E. A., Macatangay, R., Machida, T., Matsueda, H., Moore, F., Morino, I., Park, S., Robinson, J., Roehl, C. M., Sawa, Y., Sherlock, V., Sweeney, C., Tanaka, T., and Zondlo, M. A.: Calibration of the Total Carbon Column Observing Network using aircraft profile data, *Atmos. Meas. Tech.*, 3, 1351–1362, <https://doi.org/10.5194/amt-3-1351-2010>, 2010.
- Wunch, D., Toon, G. C., Sherlock, V., Deutscher, N. M., Liu, C., Feist, D. G., and Wennberg, P. O.: The Total Carbon Column Observing Network's GGG2014 Data Version, p. 43, <https://doi.org/10.14291/tccon.ggg2014.documentation.R0/1221662>, 2015.
- Yang, Z., Toon, G. C., Margolis, J. S., and Wennberg, P. O.: Atmospheric CO<sub>2</sub> retrieved from ground-based near IR solar spectra, *Geophys. Res. Lett.*, 29, 53-1–53-4, <https://doi.org/10.1029/2001GL014537>, 2002.
- Yokota, T., Yoshida, Y., Eguchi, N., Ota, Y., Tanaka, T., Watanabe, H., and Maksyutov, S.: Global Concentrations of CO<sub>2</sub> and CH<sub>4</sub> Retrieved from GOSAT: First Preliminary Results, *Sola*, <https://doi.org/10.2151/sola.2009-041>, 2009.
- Yver Kwok, C., Laurent, O., Guemri, A., Philippon, C., Wastine, B., Rella, C. W., Vuillemin, C., Truong, F., Delmotte, M., Kazan, V., Darding, M., Lebègue, B., Kaiser, C., Xueref-Rémy, I., and Ramonet, M.: Comprehensive laboratory and field testing of cavity ring-down spectroscopy analyzers measuring H<sub>2</sub>O, CO<sub>2</sub>, CH<sub>4</sub> and CO, *Atmos. Meas. Tech.*, 8, 3867–3892, <https://doi.org/10.5194/amt-8-3867-2015>, 2015.
- Zhou, M., Vigouroux, C., Langerock, B., Wang, P., Dutton, G., Hermans, C., Kumps, N., Metzger, J.-M., Toon, G., and De Mazière, M.: CFC-11, CFC-12 and HCFC-22 ground-based remote sensing FTIR measurements at Réunion Island and comparisons with MIPAS/ENVISAT data, *Atmos. Meas. Tech.*, 9, 5621–5636, <https://doi.org/10.5194/amt-9-5621-2016>, 2016.
- Zhou, M., Langerock, B., Vigouroux, C., Wang, P., Hermans, C., Stiller, G., Walker, K. A., Dutton, G., Mahieu, E., and De Mazière, M.: Ground-based FTIR retrievals of SF<sub>6</sub> on Reunion Island, *Atmos. Meas. Tech.*, 11, 651–662, <https://doi.org/10.5194/amt-11-651-2018>, 2018.